KASDI- MERBAH OUARGLA UNIVERSITY

FACULTY OF APPLIED SCIENCES

MECHANICAL ENGINEERING DEPARTMENT

Master's thesis

Specialty:Mechanical Engineering

Option: Energetic

Presented by:

HALIMI Soufiane &MOUISSI Faras Madjdi

Theme:

Optimized parameters of an air solar collector for drying applications using the experimental design method

Jury:

Dr. MENNOUCHE Djamel	University of KM Ouargla	President
Dr. BELAHYA Hocine	University of KM Ouargla	Examiner
Pr. BOUBEKRI Abdelghani	University of KM Ouargla	Supervisor
M. BENHAMZA A. Rahmane	University of KM Ouargla	Co-Supervisor

Academic year: 2017 /2018

ACKNOWLEDGEMENT

The present work was carried out as part of the thesis of academic Master in energy in the Department of Mechanical Engineering and was hosted in the Laboratory of development of new and renewable energies in arid zones (LENREZA) at the university KASDI MERBAH Ouargla (Algeria).

We would like to begin by thanking Professor **BOUBEKRI Abdelghani**, who has had the kind willingness to propose and lead this work.

We also thank gentlemen, Dr. MENNOUCHE Djamel and Dr. BELAHYA Hocine for having kindly agreed to judge this master thesis work.

Our thanks are also particularly addressed to Mr. BANHAMZA Abderrahmane for his active participation in the follow-up of this work and his constructive advice throughout the semester.

We also thank all the training teams who participated in their efforts and advice during our training course in the Department of Mechanical Engineering.

Finally, our heartfelt thanks are addressed to any person who has participated or helped, by far or near, the completion of this work.

Dédicaces:

I dedicate this modest work:

To my parents, with all my gratitude and gratitude

for their sacrifices.

To my grandparents to my uncles and aunts

To my brother ISLAM

To all my family

To all my teachers each with his name,

To all my friends and in particular: HOTHAIFA,

FAROQUE, DHIA, SALAH

To my cousin HOUSSAM

HALIMI Soufiane

I dedicate this memory:

To my parents with all my affections, and love to my familie

MOUISSI

To my collages in promo 2017/2018 mechanical energy

specially applied energetic (academic).

To all who know me I dedicate this modest work.

MOUISSI Fares Madjdi

Chaptre01: Bibliographic study in solar air collector

Chaptre02: Presentation of DOE and work software

List of figures:

List of tables:

Nomenclature

A	[m²]	Total collector array aperture or gross area (consistent with $F_R(\tau\alpha)$,$F_R U_L$,$F_R U_{L/T}$ and G_{test})
A_a	[m²]	Aperture area of a single collector module
A_r	[m²]	Absorber area of a single collector module
a_0	[-]	Intercept (maximum) of the collector efficiency
a_0	[kJ/h-m²-K]	Negative of the first-order coefficient in collector efficiency equation
a_2	[kJ/h-m²-K²]	Negative of the second-order coefficient in collector efficiency equation
b_0	[-]	Negative of the 1st-order coefficient in the Incident Angle Modifier curve
b_1	[-]	Negative of the 2nd-order coefficient in the IAM curve fit equation
C_{pf}	[kJ/kg-K]	Specific heat of collector fluid
C_{min}	[kJ/h-K]	Minimum capacitance rate (mass flow times specific heat) of heat exchanger flow streams
F_R	[-]	Overall collector heat removal efficiency factor
F_{av}	[-]	Modified value of F_R when the efficiency is given in terms of T_{av}, not T_i
F_o	[-]	Modified value of F_R when the efficiency is given in terms of T_o, not T_i
I	[kJ/h-m²]	Global (total) horizontal radiation
I_d	[kJ/h-m²]	Diffuse horizontal radiation
I_T	[kJ/h-m²]	Global radiation incident on the solar collector (Tilted surface)
I_{bT}	[kJ/h-m²]	Beam radiation incident on the solar collector
$\dot{m}$	[kg/h]	Flowrate at use conditions

$\dot{m}_{test}$	[kg/h]	Flowrate in test conditions
N_s	[-]	Number of identical collectors in series
$\dot{Q}_U$	[kJ/h]	Useful energy gain
T_a	[°C]	Ambient (air) temperature
T_{av}	[°C]	Average collector fluid temperature
T_i	[°C]	Inlet temperature of fluid to collector
T_o	[°C]	Outlet temperature of fluid from collector
U_L	[kJ/h-m²-K]	Overall thermal loss coefficient of the collector per unit area
$U_{L/T}$	[kJ/h-m²-K²]	Thermal loss coefficient dependency on T
α	[-]	Short-wave absorptance of the absorber plate
β	[°]	Collector slope above thehorizontal plane
θ	[°]	Incidence angle for beam radiation
ρ_g	[-]	Ground reflectance
τ	[-]	Short-wave transmittance of the collector cover(s)
$(\tau\alpha)$	[-]	Product of the cover transmittance and the absorber absorptance
$(\tau\alpha)_b$	[-]	$(\tau\alpha)$ for beam radiation (depends on the incidence angle θ)
$(\tau\alpha)_n$	[-]	$(\tau\alpha)$ at normal incidence
$(\tau\alpha)_s$	[-]	$(\tau\alpha)$ for sky diffuse radiation
$(\tau\alpha)_g$	[-]	$(\tau\alpha)$ for ground reflected radiation

GENERAL INTRODUCTION

Energy is the main source of human history since ancient times, as it has been harnessed according to its needs. The energy of several forms and types, including fossil energy and nuclear energy, has been used by humans in all industrial, economic and other fields. However, this energy has been damaged and has been problematic as energy consumption has increased in recent times. Fossil energy is being threatened by the use of the world's extraordinary usage. This has led to an environmental imbalance and many problems. So, the world's orientation towards renewable energies is justified as it is considered clean energies and has many forms.

Solar energy is a kind of clean renewable energy. It is an inexpensive energy to get it and it is available during the course of the year. Solar thermal energy can be converted to electrical energy, which is known as photovoltaic and thermal energy to heat through used fluid (water or air). They can be converted to any type of energy as needed.

Solar thermal energy is the instantaneous transformation of the energy of solar rays into thermal energy. This transformation can be used directly, for example the heating of sanitary water using solar collectors, or indirectly in the case of the production of electricity in a solar thermodynamic plant. The solar thermal is based on the use of heat transmitted by radiation that is different from that of photovoltaic where electricity is generated by the energy of photons. With the help of technological advances, the techniques of direct capture of some of the solar energy are significantly improved in order to make the solar systems more reliable, efficient and profitable [1]. The easiest way to utilize solar energy for heating applications is to convert it into thermal energy by using solar collectors. Solar air heater is one such method to convert solar energy to thermal energy. Thermal efficiency of solar air heater is less due to low heat transfer capability between absorber plate and fluid flowing in the duct. Double pass solar air heaters have large area for heat absorption hence thermal efficiency increases [2].

We also know that winter has low temperatures and solar radiation, compared to summer. This has a negative impact on the efficiency of the solar collector in terms of heat acquired by a collector through solar radiation. It is also difficult to afford exorbitant costs for making many solar collection models, looking for a better experience and wasting time in the manufacturing period. That is why we want to go to numerical

simulation, where it is inexpensive and also allows us to create many experiments in a short and fast time.

Our study aims to improve the performances of solar air collector for use in indirect solar dryers. We have to look at the factors we can control how much taking into consideration. To do so, we will adopt a solving methodology based on energetic calculations coupled to experimental design method. This approach needs the use of numerical tools: TRNSYS software, STATGRAPHICS and METEONORM.

The present manuscript is organized through an introduction, four chapters and a general conclusion. In the first chapter, we discussed the relevant details about the compounds and the characteristics of each element, in terms of influencing the collector and the factors influencing it and also the types of solar collectors and their uses. In chapter 2, we have described the principle of the functioning of numerical simulation tools and their basic concepts. As for chapter 3, we have explained the steps we have followed while running each of the used programs. Finally, chapter 4 presents the important and relevant results issued from this study.

Chapitre 01:

Bibliographic study on solar air collector

1.1.Solar thermal energy :

Solar thermal energy is the direct use of solar energy. It is the instantaneous conversion of sunlight energy into thermal energy. This transformation can be used directly as domestic hot water using solar collectors, or indirectly in the case of producing electricity in a solar thermodynamic plant [3].

Solar thermal energy has many applications:

- domestic hot water;
- home heating;
- heating swimming pool water;
- crop drying; absorption refrigeration for buildings;
- producing high temperature.

1.2. Solar thermal collector

1.2.1. Definition :

The solar thermal collector is the principal element in solar energy systems This device is a heat converter which absorbs the incoming solar radiation and converts it into heat to transfers this heat energy to a heat transfer fluid usually we use: (air, water, or oil) flowing through the collector. The energy gain is the difference between the absorbed solar energy and the losses from the collector the losses are of three types, conduction, convection and radiation [4].

The solar energy thus collected is carried from the circulating fluid either directly to the hot water or space conditioning equipment or to a thermal energy storage tank from which can be drawn for use at night and/or cloudy days [5].

1.2.2. Solar collector types :

There are two mainly types of solar thermal collector:

- non-concentrating collector:

it Utilizes the whole collector space, for intercepting and absorbing solar radiation

- concentrating collector:

usually has concave reflecting surfaces to intercept and focus the sun's beam radiation to a smaller receiving area, thereby increasing the radiation flux [4].

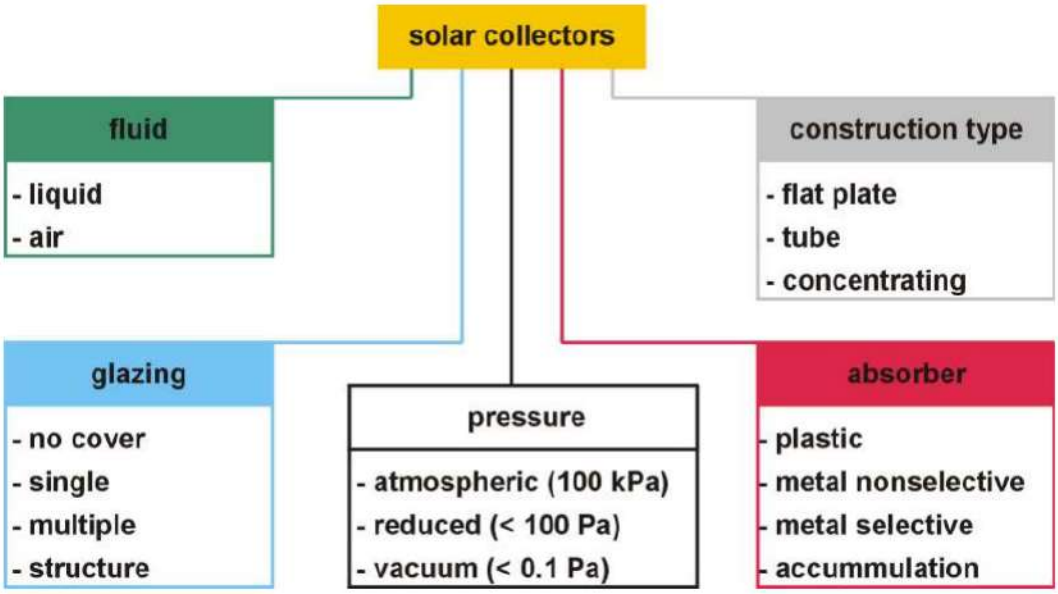

Figure 1. 1: General types of solar thermal collector [6]

1.2.2.1. Parabolic solar collector:

Solar concentrator is a device which concentrates the solar energy incident over a large surface onto a smaller surface. A solar collector consists of a concentrator and a receiver. There are three alternative configurations of concentrators [7].

- Parabolic trough concentrators;
- Solar power towers (Central receiver concentrators);
- Parabolic dish concentrators.

1.2.2.2. plat flat solar thermal collector:

Flat-plate solar collectors have potential applications in many space-heating situations, air conditioning, industrial process heat, and also for heating domestic water. They are usually fixed in position permanently, have fairly simple construction, and require little maintenance and, the wavelength range of importance for flat-plate solar collectors is from the visible to the infrared [8].

a. water solar plat flat collector:

Flat-plate collectors are the most common solar collector for solar water-heating systems [9]. The collector therefore is the link between the sun and the hot water system [10] in homes and solar space heating. A typical flat-plate collector consists of an absorber, transparent cover sheets. Usually (glass) one or more transparent covers, and an insulated box. The absorber is usually a sheet of high-thermal conductivity metal with tubes or ducts either integral or attached. Its surface is painted or coated to maximize radiant energy absorption and, in some cases, to minimize radiant emission. The insulated box provides structure and sealing and reduces heat loss from the back or sides of the collector [5]

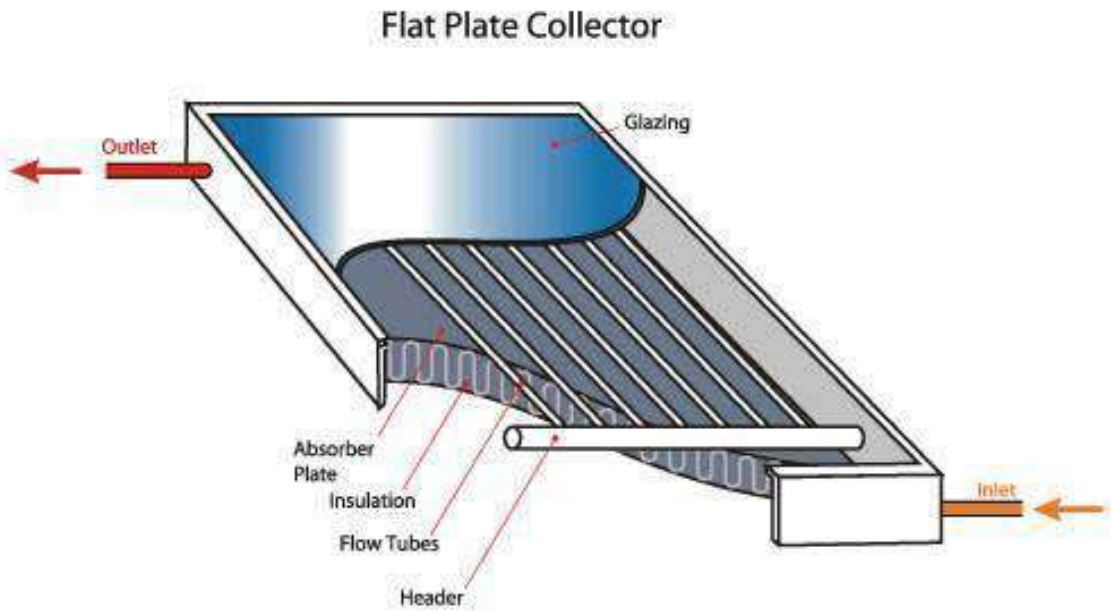

Figure 1. 2: A Flat plate solar water collector [11]

1.3. Solar air plat flat collector:

1.3.1. Definition :

Flat plate solar air heaters are usually applied in space heating and drying processes of agricultural products, herbal medicines, clothing etc. This system occupies an important place among solar thermal systems because of minimal use of materials [12]. The design, construction materials and construction methods for solar air heaters have been slowly developed compared to liquid-based collectors. The efficiency of air collectors is lower because of low thermal capacity of air and low absorber-to-air heat transfer coefficient. The most important advantages for air type collectors include: no freezing or pressure problems; generally lower construction cost. [13]. The absorber plates in air collectors can be metal sheets, layers of screen, or non-metallic materials. Air collector absorber plates can be unfilled or wavy to create air turbulence that helps the heat to pass from the plate. The air flows through the absorber by natural convection or it is forced by a fan [5].

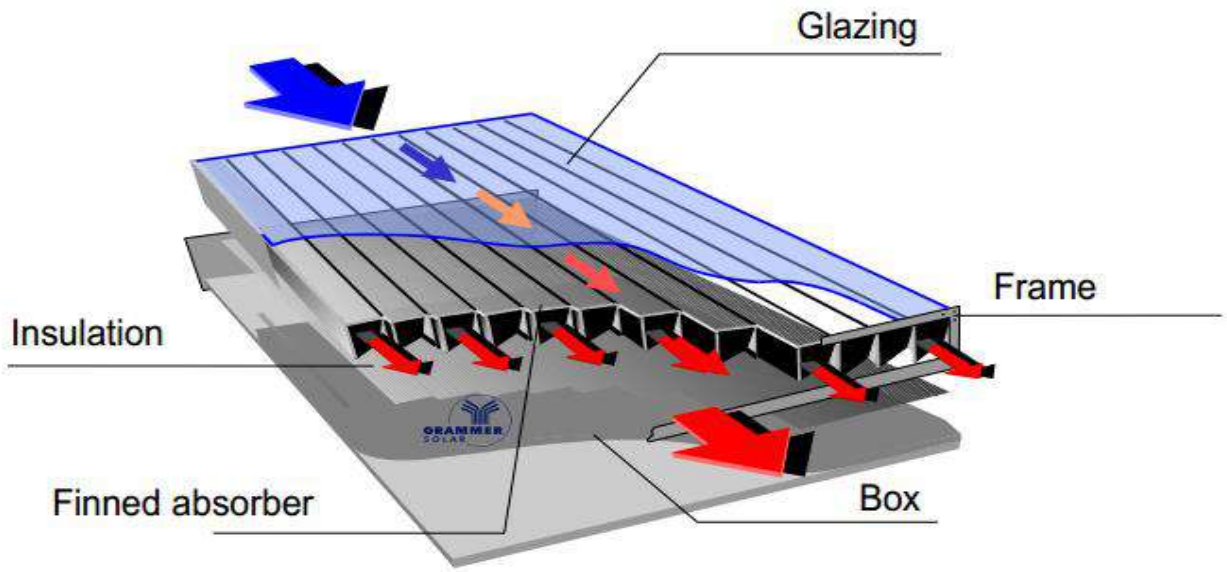

Figure 1.3: Solar air collector plat flat [6]

1.3.2. Classification of Double Pass Solar air heaters:

Different types of air flow channel configuration are given below. Each configuration gives different outlet temperature and thermal efficiency.

1.3.2.1. Double Flow Single Pass Solar air heater:

Two channels are provided in 'double Flow Single Pass' solar air heater. Upper channel is between glass cover and absorbing plate and bottom channel is between absorbing plate and lower insulation. Air approaching the double pass solar air heater is bifurcated and one part goes in upper channel while other goes to bottom channel simultaneously as shown in figure (1.4). For both channels air enters and directly leaves without any turn and hence its name "double flow single pass". It has greater heat transfer area and thermal efficiency compared to single pass solar air heater [14]

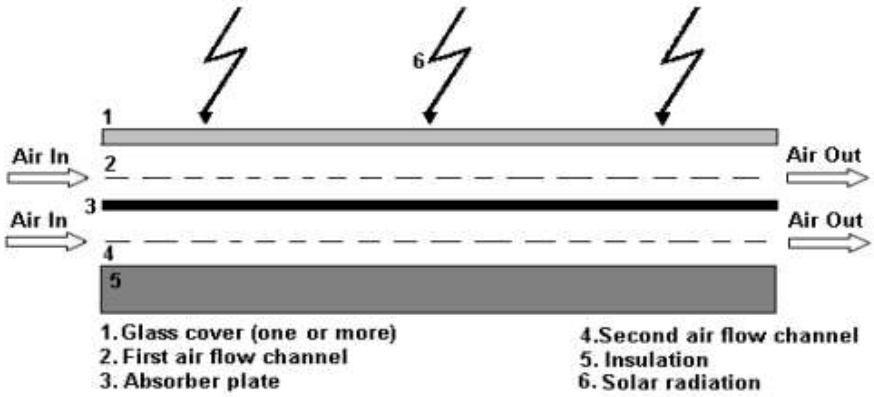

Figure 1.4: A schematic view of double flow single pass [14]

1.3.2.2. Single Flow Double Pass Solar air heater:

Single flow double pass solar air heater also has two channels for air flow. Upper channel is between glazing and absorbing plate and bottom channel is between absorbing plate and lower insulation as shown in Figure (1.5). Air enters the upper channel, changes direction by 180o at the end and leaves the air heater through bottom duct. There are two variants for this type of flow configuration. In the first design, two channels are separated by a glass cover and

absorbing plate is below the bottom channel. In the second design, two channels are separated by absorbing plate and glass cover is above the upper flow channel. [14]

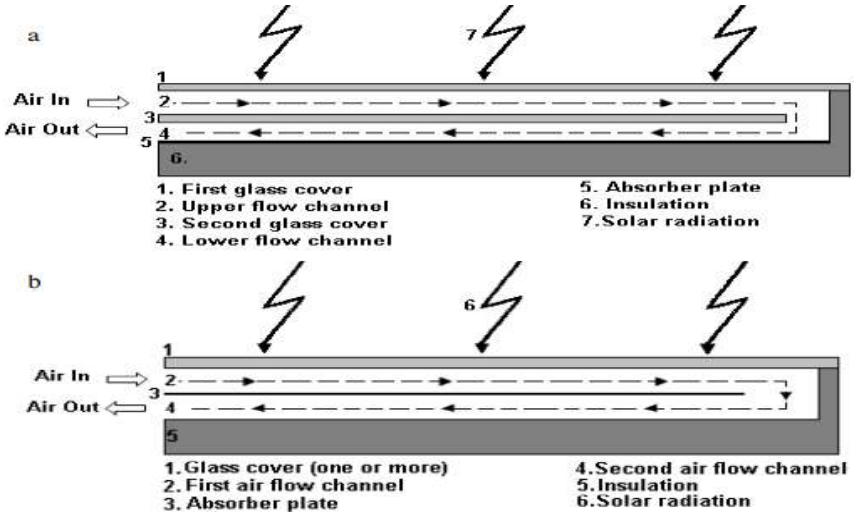

Figure 1.5: Schematic view of single flow double pass [14]

1.3.2.3. Single Flow Recycled Double Pass Solar air heater:

These types of heaters are used when temperature outlet desired is constant. A part of flow is recycled back to the inlet so that outlet temperature can be controlled. A schematic diagram is show in Figure (1.6). Recycling the air results in improve in thermal efficiency as reported in literature. Solar air heaters also consist of two channels. The upper channel is formed between glass cover and absorbing plate. While bottom channel is formed between absorbing plate and lower insulation. Air enters and leaves the upper channel in same direction and hence its name 'Single pass'. Two channels are present which justify the name as 'Double pass' [14].

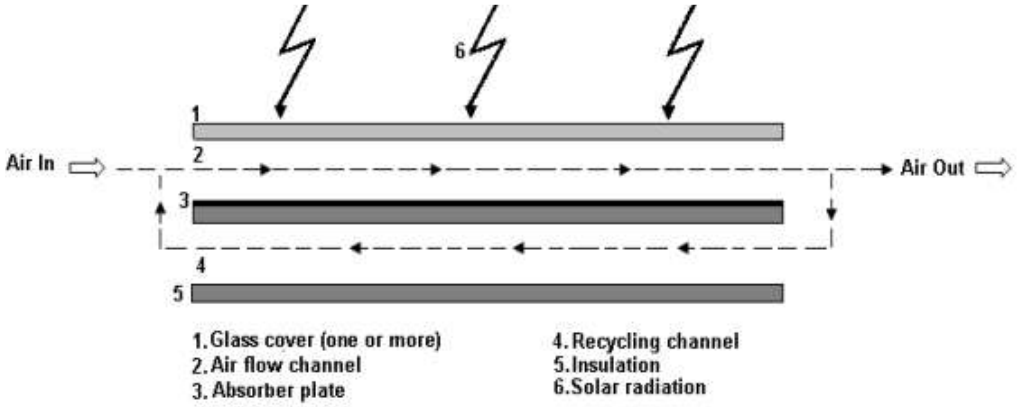

Figure 1.6: A schematic view of single flow recycled double pass [14].

1.3.3. The different components of a solar air collector:

The solar air collector consists of the following elements

- The Glass cover
- The Absorber
- The insulation
- The Cover
- The Heat transfer fluid

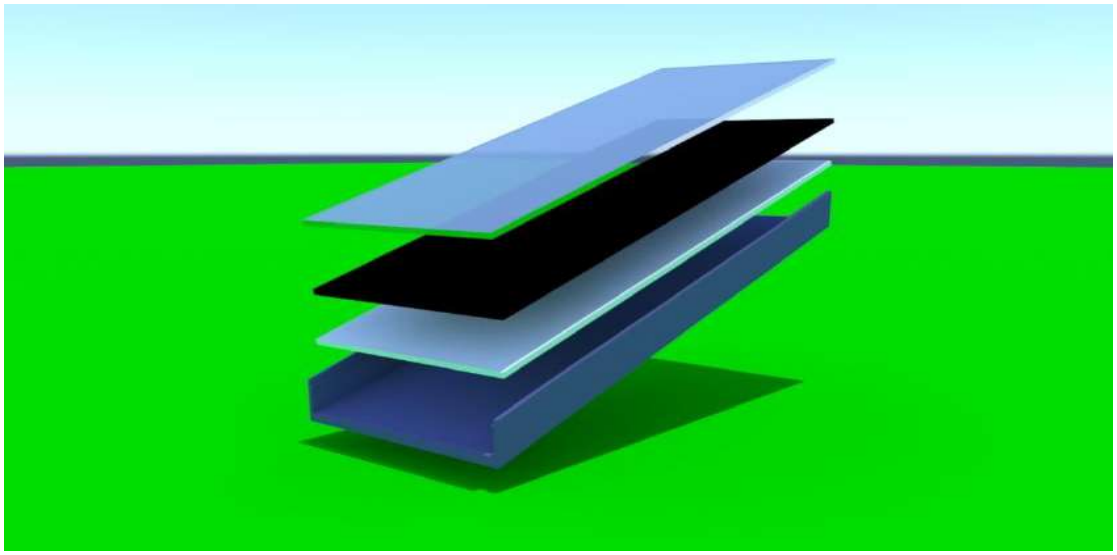

Figure 1.7: Solar air collector 3D

1.3.3.1. The Glass cover:

Usually used over the top of the absorber. Glass is used to stop convection on the top side because it allows the solar radiation to pass through to the absorber plate. [18]

Table 1.1 : Properties of some surfaces transparent to solar radiation but Opaque to infrared radiation [13]

Material	Factor of Transmission Solar (%)	Density (kg/m3)	Mass heat (J/kg.K)	Thermal conductivity (w/m.K)	Thermal expansion (K-1)
Glass	85-92	2700	840	0.93	0.9 10-5
Polycarbonate	82-89	1200	1260	0.2	6.6 10-5
Polyméthacrylate	89.92	1200	1460	0.2	7 10-5
Armed polyester	77.90	1400	1050	0.21	3.5 10-5
Polytéréphtalate ethylene	84	1.38	1170	0.25	7 10-5
Polyfluoroéthyléne Opoyléne	97	2.15	1170	0.25	10-4
Polyflurure Vinyl	93	1.50	1380	0.12	4 10-5

1.3.3.2. The Absorber:

Is made from a material which can rapidly absorb heat from the sun's rays. It is usually made from black painted metal (copper, steel, aluminum, or plastic….ect) to maximize absorption and minimize reradiation [16] and also The best coefficients are in the order of 0.95 [17].The absorber must perform the following functions [18]:

- Absorb the greater part of the incident radiation.
- Transmit heat produced by this absorption to the heat transfer fluid

Table 1. 2: Thermo-Physical characteristics of metallic materials [13]

Metal	Thermal conductivity (w/m.K)	Mass heat (J/kg.K)	Density (kg/m3)	Diffusivity (10-6 m2/s)
Copper	384	398	8900	108
Stainless Steel	14	460	7800	04
Aluminum	204	879	2700	86

The absorber must not be too thin. In practice, a sheet of copper or aluminum of 0.2 mm thickness is usually used with variants of 0.15 to 0.3 mm [19]

1.3.3.3. The insulation:

The transfer of thermal energy takes place from a higher to lower intensity and can be chieved by using a convection or a conduction or by radiation process. In the case of heat, it can be transferred by both processes. In order to prevent the undesired transfer of heat, the material must be designed with a shielding property called insulation material. Its basic function is to prevent heat transfer from inside solar thermal systems to the outside environment.

The most commonly used insulating materials are:

1. **Organic group:** Cellular glass, glass wool with bers.
2. **Inorganic group:** Polystyrene, sheep wool, cotton wool, polyester ber.
3. **Combined material:** Glued Expanded polystyrene board, wool, wood board, wood ber board the section refers to source [20].

Table 1.3: Thermal properties of some insulating materials [15]

Metal	Thermal conductivity (w/m.K)	Density (kg/m3)	Mass heat (J/kg.K)	Diffusivity (10-7 m2/s)
Air (at 20°C)	0.025	1.2	1003	208
Polyurethane foam	0.029	30	1600	6.0
Glass wool	0.036	40	840	10.7
Polystyrène Expansé	0.040	20	1500	13.3
Compressed newsprint	0.105	130	1340	6.0

1.3.3.4. The Cover:

It is made of metal, wood or solid plastics and must be resistant to shocks and also prevents any physical damage from extreme weather conditions. and also, be easy to decipher and install to repair any problem that can happen to the complex.

1.4. Drying :

1.4.1. Introduction :

Drying is generally used to remove moisture or liquid from a wet solid by converting this moisture into gaseous state. In most drying operations, water is the liquid evaporated and air is normally employed as drying gas [3.21]. In many practical applications, drying is a process which requires high energy input because of the high latent heat of water evaporation and relatively low energy efficiency of industrial dryers. It is reported that industrial dryers consume on average about 12% of the total energy used in industrial processes [3.22]. In those processes where drying is required, the cost of drying can approach to 60-70% of the total cost [19-23]. Drying equipment may be classified in several ways. The most common classification is based on the mode of heat input. The heat needed for drying is supplied to the material by one of the following methods [16-23]: radiation drying; convective drying (using a drying medium, air); contact drying (by conduction from a surface that is in direct contact with the material to be dried).

1.4.2. Classification of Solar Dryers :

A classification chart of drying equipment on the basis of heat transfer is shown in Figure 5.2 [24-25]. This chart classifies dryers as direct or indirect, with subclasses of continuous or batch wise operation. Solar energy drying systems are classified primarily according to their heating modes and the manner in which the solar heat is utilized [26]. In broad terms, they can be classified into two major groups, namely:

- passive solar-energy drying systems (conventionally termed natural-circulation solar drying systems)

- active solar-energy drying systems (most types of which are often termed hybrid solar dryers).

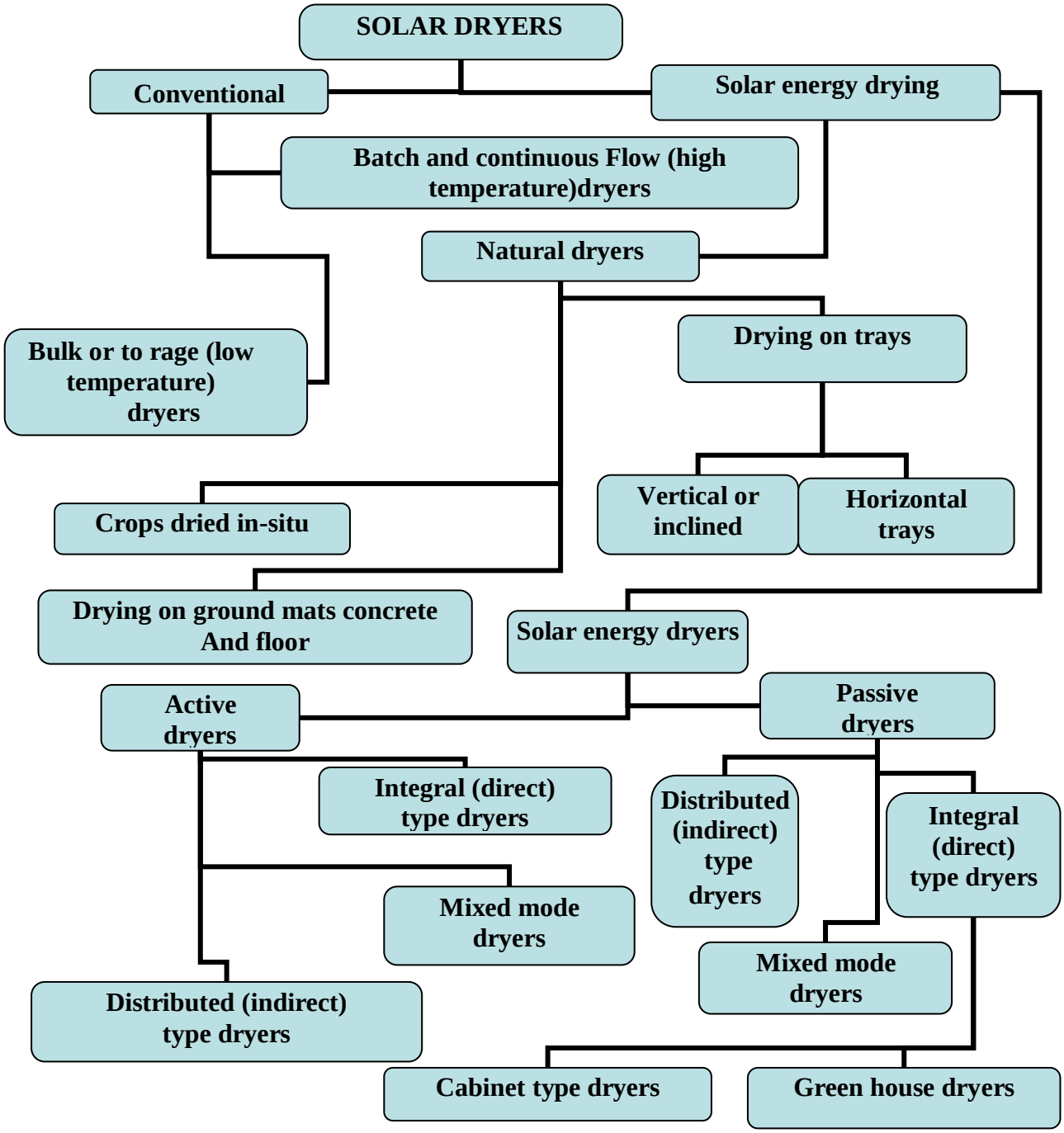

Figure 1.8: Classifications of dryers and drying modes [24].

1.4.3. Types of Solar Dryers :

Solar energy dryers can broadly be classified into direct, indirect and hybrid solar Dryers and have to kind passive drying and active dryers

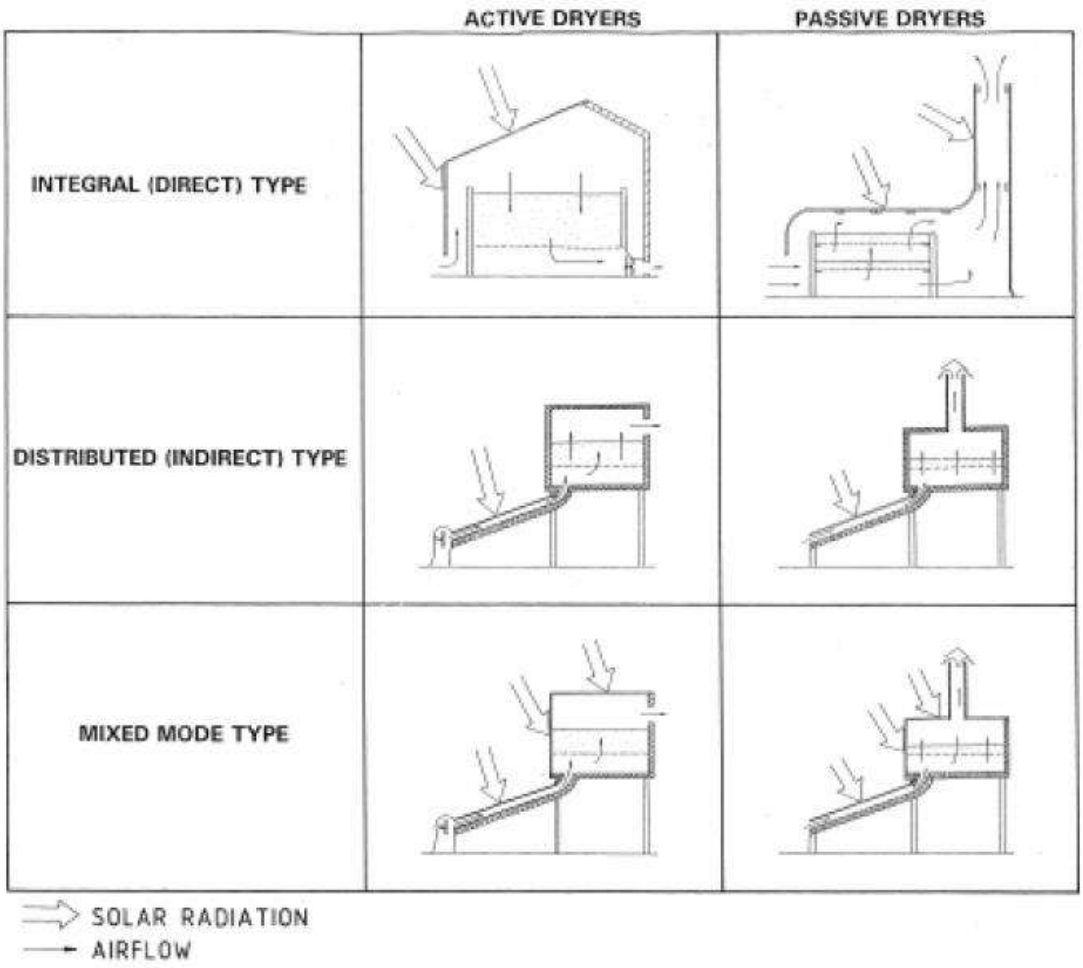

Figure 1.9: Typical solar energy dryer designs [24]

1.4.3.1. Direct Solar Dryer:

In a direct solar dryer, the products are directly exposed to the solar radiations. As shown on Figure 5.4, a solution is to put the products under a transparent cover such as glass or plastic. The advantage of such a method is its simplicity and low price since material and maintenance require low investment. [27] The solar radiation arrives on the glass cover and

heats up the air which circulates either naturally (passive solar dryer) or by wind pressure using external sources (active solar dryer) or both [26].

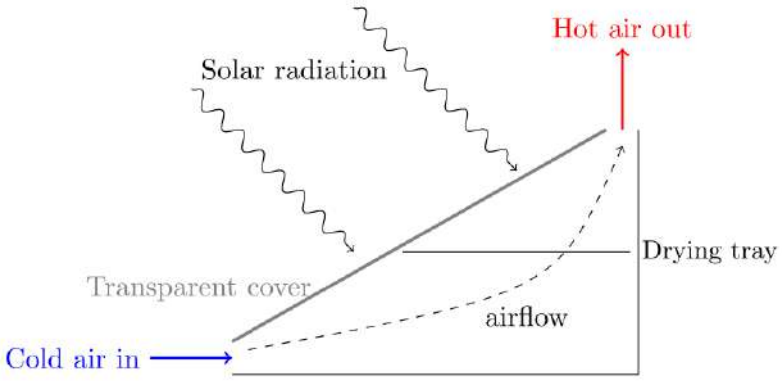

Figure 1. 10: Design of a direct solar dryer

1.4.3.2. Indirect solar dryer:

The indirect solar drying working principle relies on the use of solar radiation by a solar collector to heat air, and the product to be dried is not directly exposed to solar radiation so it is possible to avoid the discoloration of the product [29-30] and vitamines degradation. These solar dryers include the following components:

- an air-heating solar collector
- a drying chamber
- eventually a chimney

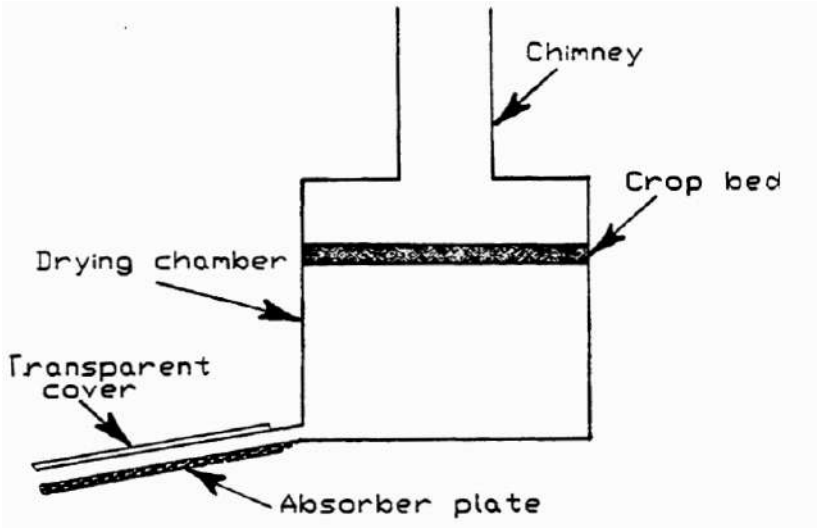

Figure 1.11: Typical natural convection indirect solar dryer with a chimney [30]

1.4.3.3. Mixed Mode Solar Dryers:

A mixed solar dryer working principle aims to use solar radiation for both direct heating of the product and preheating of air thanks to a spare energy source such as solar energy or biomass heater [31]. Figure 5.5 presents an example of a hybrid passive solar dryer. This model is very similar to a classic passive indirect solar dryer except that the drying chamber's walls are made of glass so the direct solar radiation can impinge the product to be dried [32]

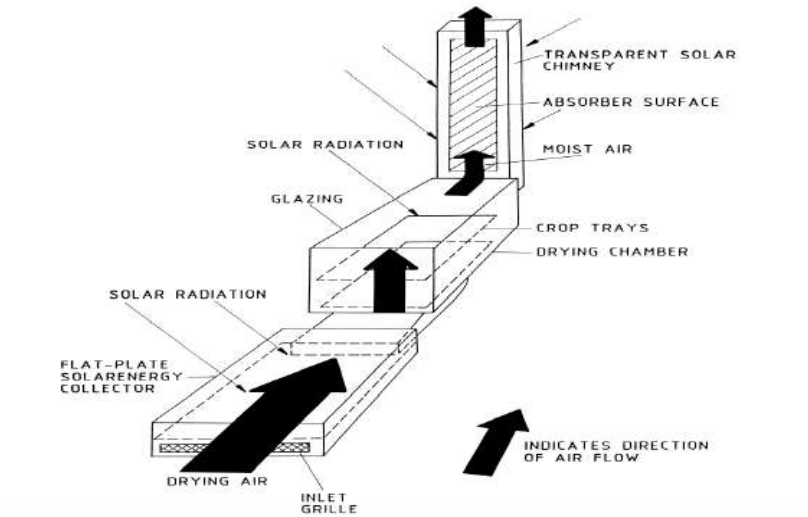

Figure 1.12: Design of a passive hybrid solar dryer [32]

Chapter 02:

Presentation of DOE and work software

2.1.**Introduction:**

In this chapter, we will provide a brief explanation about the programs that we will use in the next chapter, where we will refer to the introduction of the software TRNSYS and the presentation of its negatives and its pros, and we will also explain the mathematical way in which we study for examples and the range of digital programs used in this field. Focusing on the software STATGRAPHICS that we have adopted in our study.

2.2. **Design of experiments**

Traditional method of experiments (the method of abstract and error experiment), which is usually based on changing the coefficient after another, to watch the change with time, that does not gives satisfactory results of overlapping (links) between different factors, which directly affect the experience, as well as the length of trials [32], in order to eliminate the disadvantages of traditional experiences, a method has emerged that relies on the least possible number of experiments by defining the relationship between the different impact factors and desired outcomes, called design of experiments.

2.2.1. **Design of Experiments Methodology**

Experimental design is how to conduct and plan experiments in order to extract the maximum amount of information from the collected data in the presence of noise. The basic idea is to vary all relevant factors simultaneously, over a set of planned experiments, and then connect the results by means of a mathematical model. This model is then used for interpretation, predictions and optimization. [33]

2.2.2. **Objectives of design of experiments**

During the investigation the following questions need to be answered: Which factors have a real influence on the responses (results)? Which factors have significant interactions (synergies or antagonism)? What are the best settings of the factors to achieve optimal conditions for best performance of a process, a system or a product? What are the predicted values of the responses (results) for given settings of the factors? An experimental design can be set up to answer all of these questions. [33]

2.2.3. **Factors**:

inputs to the process in such experiments, two types of factors are varied: Controllable factors are factors that can be controlled and whose effects are of primary interest. Noise factors are factors that

cannot normally be controlled and whose effect on the response needs to be minimized [34]. The controllable variables will be referred to throughout the material as factors. generally, Noise Factor an uncontrollable factor that causes variability under normal operating conditions, but we can control it during the experiment using blocking and randomization.

2.2.4. Levels (settings of each factor in the study):

- **Low** – for continuous or mixture factors, the low end of the range at which the factor will be set during the experiment;
- **High** – for continuous or mixture factors, the high end of the range at which the factor will be set. Levels – for categorical factors, the specific levels that will be used in the experiment. Separate each level with a comma;
- **Categorical** – a factor that can only take a discrete set of values, such as A or B;
- **Continuous** – a factor that can be varied over a continuous range;
- **Mixture** – a factor that represents the amount of a component contained in a mixture. [34]

2.2.5. Response (output of the experiment):

are measurable outcomes potentially influenced by the factors and their respective levels. Experimenters often desire to avoid optimizing the process for one response at the expense of another. For this reason, important outcomes are measured and analyzed to determine the factors and their settings that will provide the best overall outcome for the critical-to-quality characteristics - both measurable variables and assessable attributes [35].

2.3. General types of experimental design

2.3.1. Screening:

designs intended to select the most important factors affecting a response. Most of the designs involve only 2 levels of each factor. The factors may be quantitative or categorical. [34]

2.3.2. Response Surface:

These designs are intended to find the optimal levels of the experimental factors. Each factor is run at 3 or more levels. Note: response surface designs are only available if all factors are continuous. [36]

2.3.3. Multilevel Factorial

These designs allow you to specify the number of levels at which each factor is to be set and consist of all combinations of the levels of those factors. It is commonly used to generate a set

of candidate runs for selection by the D-optimal design creation procedure. Note: multilevel factorial designs are only available if all factors are continuous. [36]

2.3.4. Orthogonal Array

a general class of designs developed by Genichi Taguchi. The factors may be quantitative or categorical. [36]

2.4. Fit models

2.4.1. Mean:

If the experiment involves any process factors or if the experiment involves any mixture components, this model assumes that the factors or the components have no impact on the response. It consists of a single constant term [34]:

$$\mathbf{Y = \beta_0} \qquad (2.1)$$

2.4.2. Linear:

a. If the experiment involves any process factors, this model adds a coefficient that multiplies each factor [34]:

$$\mathbf{Y = \beta_0 + \beta_1 x_1 + \beta_2 x_2 + \beta_3 x_3} \qquad (2.2)$$

b. If the experiment involves any mixture components, this model includes a coefficient that multiplies each component [34]:

$$\mathbf{Y = \beta_1 x_1 + \beta_2 x_2 + \beta_3 x_3} \qquad (2.3)$$

2.4.3. 2-Factor Interactions:

This model adds cross-products for each pair of factors, only If the experiment involves any process factors [34]:

$$\mathbf{Y = \beta_0 + \beta_1 x_1 + \beta_2 x_2 + \beta_3 x_3 + \beta_{12} x_1 x_2 + \beta_{13} x_1 x_3 + \beta_{23} x_2 x_3} \quad (2.4)$$

2.4.4. Quadratic:

a. If the experiment involves any process factors, this model adds a quadratic term for each factor [34]:

$$\boldsymbol{Y = \beta_0 + \beta_1 x_1 + \beta_2 x_2 + \beta_3 x_3 + \beta_{12} x_1 x_2 + \beta_{13} x_1 x_3 + \beta_{23} x_2 x_3 + \beta_{11} x_1^2 + \beta_{22} x_2^2 + \beta_{33} x_3^2} \quad (2.5)$$

b. If the experiment involves any mixture components, this model adds cross-products for each pair of components [34]:

$$\mathbf{Y = \beta_1 x_1 + \beta_2 x_2 + \beta_3 x_3 + \beta_{12} x_1 x_2 + \beta_{13} x_1 x_3 + \beta_{23} x_2 x_3} \quad (2.6)$$

2.4.5. Cubic:

a. If the experiment involves any process factors, this model adds third-order terms [34]:

$$\mathbf{Y = \beta_0 + \beta_1 x_1 + \beta_2 x_2 + \beta_3 x_3 + \beta_{12} x_1 x_2 + \beta_{13} x_1 x_3 + \beta_{23} x_2 x_3 + \beta_{11} x_1^2 + \beta_{22} x_2^2 + \beta_{33} x_3^2 + \beta_{111} x_1^3 + \beta_{222} x_2^3 + \beta_{333} x_3^3 + \beta_{112} x_1^2 x_2 + \beta_{113} x_1^2 x_3 + \beta_{122} x_1 x_2^2 + \beta_{223} x_2^2 x_3 + \beta_{133} x_1 x_3^2 + \beta_{233} x_2 x_3^2 + \beta_{123} x_1 x_2 x_3} \quad (2.7)$$

b. If the experiment involves any mixture components, this model adds additional third-order terms [34]:

$$\mathbf{Y = \beta_1 x_1 + \beta_2 x_2 + \beta_3 x_3 + \beta_{12} x_1 x_2 + \beta_{13} x_1 x_3 + \beta_{23} x_2 x_3 + \beta_{123} x_1 x_2 x_3 + \delta_{12} x_1 x_2 (x_1 - x_2) + \delta_{13} x_1 x_3 (x_1 - x_3) + \delta_{23} x_2 x_3 (x_2 - x_3)} \quad (2.8)$$

2.4.6. Special cubic:

This model adds a special term involving the product of 3 components, only If the experiment involves any mixture components [34]:

$$\mathbf{Y = \beta_1 x_1 + \beta_2 x_2 + \beta_3 x_3 + \beta_{12} x_1 x_2 + \beta_{13} x_1 x_3 + \beta_{23} x_2 x_3 + \beta_{123} x_1 x_2 x_3} \qquad (2.9)$$

2.5. STATGRAPHICS

STATGRAPHICS is a general-purpose statistical package which is highly suitable for use in teaching beginning students of economics and econometrics, as well as those taking courses in business, engineering, mathematics, and other fields. Its appealing use of graphics, together with its easy-to-use menu system, make it ideal as a tool to stimulate and interest the user. This is especially true at the initial stages of a student's encounter with quantitative material, when he or she may feel some prior resistance. The package has gone through several versions, with more recent ones offering enhanced procedures, improved data-handling facilities, and a quantum leap in the quality of documentation [37].

The Experimental Design menu and associated help, usually murky areas in most generic statistics products, are particularly well-implemented. Nothing can make this work a no-brainer, but the program takes a pretty good stab at it. Although users need to have some understanding of what they are doing, the program offers good mnemonic prompts (to the basic principles, to design classes and to design creation, for instance), and the progressive dialogue makes implementation as painless as possible. Users are led through the creation, modification, optimization, augmentation and analysis of their designs in a fairly unbreakable way. The available tools successfully cover screening; response surfaces; mixtures; multilevel factorials; inner/outer arrays; single or multifactor categorical, hierarchical variance components; and multiple-response optimization. [38].

2.6. DOE in STATGRAPHICS:

The Experimental Design section of STATGRAPHICS contains a new wizard that assists users in constructing and analysing designed experiments. It guides the user through twelve important steps [36]. which can be summarized as represented in the following figure (2.1).

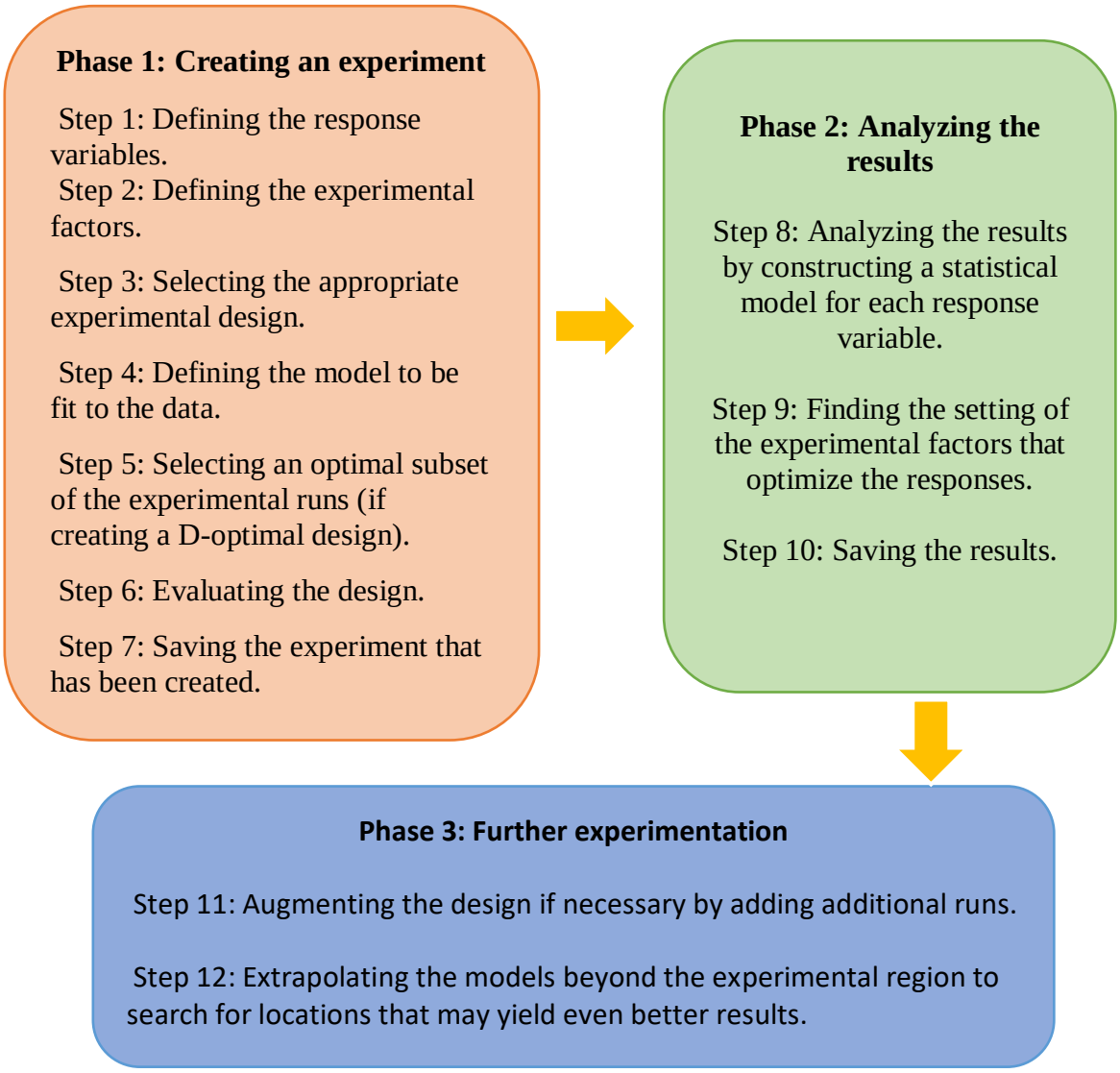

Figure 2.1: DOE steps adapted from [34]

2.7. Simulation of solar air collector by TNNSYS:

Because of the exorbitant costs and time, we lose in experimental terms. The tests are an effective way to reduce the basic challenge of time and cost as our laws can make many experiments in a short and less time. Without loss of material, let's almost give the same results as we get in real-life experiments. Many researchers have been addressing the tests to avoid problems and obstacles. TRNSYS software has been chosen for the simulation for the various advantages it presents.

2.7.1. Presentation of the Software TRNSYS:

TRNSYS is a flexible tool designed to simulate the energy performances of dynamic systems. Developed by the University of Wisconsin and the University of the Colorado in the USA, TRNSYS was initially used to simulate some components relative to the solar energy use. The

specificity of the software consists in its modular aspect. Indeed, it is built from a list of subroutines written in FORTRAN. Each subroutine models one module or type. Every type is an independent computer object. It corresponds to an element of the thermal system composed of inputs, outputs and parameters. To simulate a complete system for instance a desiccant cooling system, the user must define the different components of this system first from a library of types and connect them together in order to constitute the complete system. A graphic interface called Simulation Studio allows visualizing all components of the system. The particularity of TRNSYS amongst the others [39]. The program also owns a huge library of ingredients that make it one of the strongest and most flexible but less friendly (because of the time needed for long learning). In the following lines, the above program will be used to calculate the outlet temperature, during the day by the solar collector. After that, the results of the tests will be used for crop drying operations

2.7.2. Advantages of TRNSYS Software:

The advantages offered by the TRNSYS software are very numerous:

- Ability to change the source code itself to customize your model.
- Great opportunity to define the simulation period.
- It is extremely flexible to model a set of thermal systems at different levels of complexity
- Extensive Documentation of sub-programs (x) including explanation, common uses and basic equations. [40]

2.7.3. Disadvantages of TRNSYS Software:

- TRNSYS does not have a default value or system, so the user must have system-defined data.
- Simplifying the heat exchange gradient with a standard approach to temperature
- No error checks in the surfaces and volumes entered in the program [40]

2.7.4. Assembling a system:

The main visual interface is the TRNSYS Simulation Studio. From there, a project can be created by drag-and-dropping components to the workspace, connecting them together and setting the global simulation parameters. The Simulation Studio saves the project information in a TRNSYS Project File (*.tpf). When a simulation is run, the Studio also creates a TRNSYS input file (text file that contains all the information on the simulation but no graphical information). The simulation Studio also includes an output manager from where it can be

controlled which variables are integrated, printed and/or plotted, and a log/error manager that allow to study in detail what happened during a simulation [39].

2.7.5. Inputs and outputs:

An important step in the creation of an assembly in Simulation Studio is the specification of the required variables for each component model. With the graphical interface, outputs from one component can be connected to the inputs to another. The specific variable (input, output, parameter, and derivative) window can be accessed in the assembly panel by double-clicking the desired model icon. The Simulation Studio generates a text input file for the TRNSYS simulation engine (TRNSYS16.1). That input file is referred to as the **deck file.** During simulation output from a component is fed to the other components according to the order of the components set up in the model [39].

2.8.**METENORM:**

The METENORM software allows for TRNSYS to have reliable climatic data every hour and for a year. If one does not have a meteorological station, METENORM can calculate by interpolation between different stations the climatic conditions of a place. [41]

2.9.**Theoretical flat-plate collector (Type 73)**

This component models the thermal performance of a theoretical flat plate collector. The total collector array may consist of collectors connected in series and in parallel. The thermal performance of the total collector array is determined by the number of modules in series and the characteristics of each module. This model provides for the theoretical analyses of a flat plate. The Hottel-Whillier steady-state model is used for evaluating the thermal performance. [42]

2.9.1. Mathematical Description

A general equation for solar thermal collector efficiency can be obtained from the Hottel-Whillier equation (Duffie and Beckman, 1991) as [42]:

$$\eta = \frac{Q_u}{A\, I_T} = \frac{\dot{m} C_{pf}(T_o - T_i)}{A\, I_T} = F_R(\tau\alpha)_n - F_R U_L \frac{(T_i - T_a)}{I_T} \qquad (2.10)$$

The loss coefficient UL is not exactly constant, so a better expression is obtained by taking into account a linear dependency of UL versus (Ti-Ta):

$$\eta = \frac{Q_u}{A\, I_T} = F_R(\tau\alpha)_n - F_R U_L \frac{(T_i - T_a)}{I_T} - F_R U_{L/T} \frac{(T_i - T_a)^2}{I_T} \qquad (2.11)$$

The energy collection of each module in an array of Ns modules in series is modeled according to the Hottel-Whillier equation such that (j is the module number) [42]:

$$\dot{Q}_U = \frac{A}{N_s} \sum_{j=1}^{N_s} F_{R,j}(I_T(\tau\alpha) - U_{L,j}(T_{i,j} - T_a)) \qquad (2.12)$$

Where

$$\dot{Q}_U = \frac{N_s \dot{m}_c C_{pc}}{A U_{L,j}} \left(1 - \exp\left(-\frac{F' U_{L,j} A}{N_s \dot{m}_c C_{pc}}\right)\right) \qquad (2.13)$$

The collector fin efficiency factor, F', can be determined in a manner given in reference 2. The overall loss coefficient is a complicated function of the collector construction and its operating conditions. The following expression, developed by (Klein, 1975), is used to approximate $U_{L,j}$ in kJ/h-m2-K:

$$U_{L,j} = \frac{3.6}{\frac{N_G}{\frac{C}{T_{p,j}}\left[\frac{T_{av,j} - T_a}{N_G + f}\right]^{.33} + \frac{1}{h_w}}} + \frac{3.6\,\sigma\left({T_{av,j}}^2 + {T_a}^2\right)\left(T_{av,j} + T_a\right)}{\frac{1}{\varepsilon_p + .05N_G(1 - \varepsilon_p)} \frac{2N_G + f - 1}{\varepsilon_g} - N_G} + U_{be} \qquad (2.14)$$

Where

$$h_w = 5.7 + 3.8W\ [w/m^2k] \qquad (2.15)$$

$$f = (1 - 0.04\,hw + 0.0005\,hw^2)(1 + 0.091N_G) \qquad (2.16)$$

$$c = 365.9(1 - 0.00883\,\beta + 0.0001298\,\beta^2) \quad (2.17)$$

The overall transmittance-absorptance product is determined as:

$$(\tau\alpha) = \frac{I_{bT}(\tau\alpha)_b + I_d\left(\frac{1+\cos\beta}{2}\right)(\tau\alpha)_s + \rho I\left(\frac{1-\cos\beta}{2}\right)(\tau\alpha)_g}{I_T} \quad (2.18)$$

The transmittance-absorptance products for beam, sky diffuse, and ground diffuse radiation are determined with function routine TALF . Effective incidence angles for sky diffuse and ground reflected radiation are as defined in the mode l collector description. The outlet temperature of one module is used as the inlet to the next and is given as:

$$T_{o,j} = \frac{AF_{R,j}(I_T(\tau\alpha) - U_{L,j}(T_{i,j} - T_a)}{N_s \dot{m}_c C_{pc}} + T_i \quad (2.19)$$

If the collector flow is zero, the collector stagnation temperature is:

$$T_p = \frac{I_T(\tau\alpha)}{U_L} + T_a \quad (2.20)$$

Chapter 03:

Presentation of the methodology of work

3.1. Introduction

In this chapter we will present all of what we have done in our study validation, optimisation and simulation process and all the elements and steps we have adopted through our reliance on STATGRAPHICS and TRNSYS software.

3.2. Validation methodology:

After getting the experimental results from the L.E.N.R.E.Z.A laboratory that was made by (HLASSA) [43] show in figure (3.1), and in order to validate it with the results of the numerical simulation using the TRNSYS software and we have chosen the appropriate simulated solar collector type for our study, which took a long time because there was no special type For air, we've chosen Type 73 as a very appropriate type for our study, this type models the thermal performance of a theoretical flat plate collector and provides for the theoretical analyses of a flat plate. And in order to introduce the boundary conditions which are the inlet flow rate, the solar radiation, the ambient, temperature and the temperature in the entrance of the solar collector, we chose Type 3a, Type 14h and Type 14e, after completing the selection of the appropriate types we have launched on validation and this is shown in the following figure (3.2).

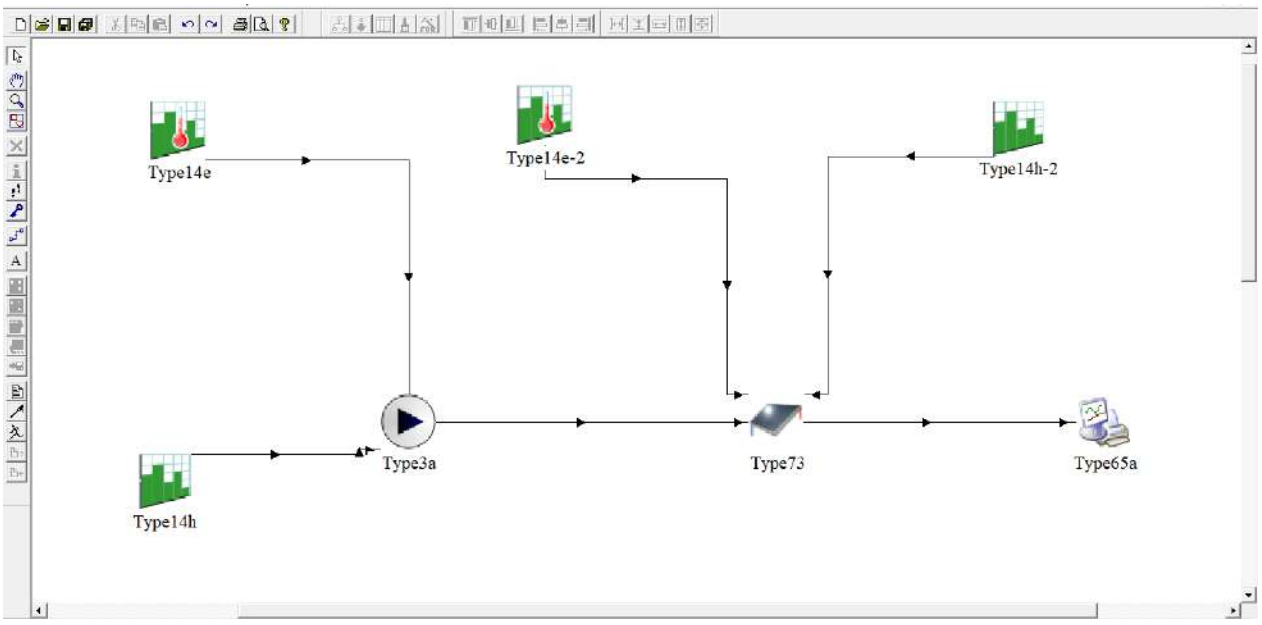

Figure 3. 1: Installation of components to match validation

3.2.1. Design and realization of the air flat plane collector

The test bench used for the test run includes an air plant sensor with a Simple pass.

Figure 3. 2: Solar air collector made by laboratory L.E.N.R.E.Z.A [43]

3.2.2. Air flat plane collector design:

The solar collector is an air- flat plane collector, surface of 2.2080 m2. Length of 1.92 m and 0.45 m in width with 0.17m of height. The sensor is covered with a glass plate, and a 0.07 m air slide is. Deposited with a matt black painted galvanized iron plate that serves as an absorber. The lateral and lower bets are thermally insulated with two layers of glass wool on the lower surface of the collector of 0.07 m thickness, the collector is inclined at an angle of 31 ° (the altitude of the city of Ouargla) in relation to the horizontal plane and oriented towards the South plane.

3.2.3. Fitted types for validation:

3.2.3.1. Type 73:

This type represents the role of a flat plat solar collector in program TRNSYS, was chosen because it contains an important number of parameters that fit for our study of the solar air collector which shown in table (3.1), this is what characterizes it from the rest of the solar collector types in the TRNSYS software and, about the variables it contains. We then entered the design parameters values of the experimental solar collector taken from the Laboratory LENREZA (collector area,

fluid specific heat, collector fin efficiency factor, absorber plat emittance, absorptance of absorber plate, index of refraction of cover, Extinction coefficient thickness product)

Remarque: we've set the value of the collector fin efficiency factor at 0.25 as default. And the index of the glass is 1.526, and for plexiglass is 1.49 [44]. And we've calculated the Extinction coefficient and the thickness product whit the following equation:

$$KL = K \times L \tag{3.1}$$

KL: Product of extinction coefficient and thickness for cover

K: the glazing extinction coefficient, witch its general value is 32.

L: the glazing thickness.

Table 3. 1: Type 73 parameter list

Nr	Name	unit	Range
1	collector area	m^2	[0; inf]
2	fluid specific heat	$kJ/kg.K$	[0; inf]
3	collector fin efficiency factor	**[-]**	[0;1]
4	absorber plat emittance	**[-]**	[0;1]
5	absorptance of absorber plate	**[-]**	[0;1]
6	index of refraction of cover	**[-]**	[0; inf]
7	Extinction coefficient thickness product	**[-]**	[0;1]

3.2.3.2. Type 14h:

After finishing the input of the values for the design parameters of the solar collector, we then entered the initial conditions, and started with the solar radiation in function of time using the type14h type, this type helps us to introduce the measured values of solar radiation and the time it was specifically measured, and in this next figure (3.2) shows how this type works in terms of time and how the measured radiation changes through the experimental results.

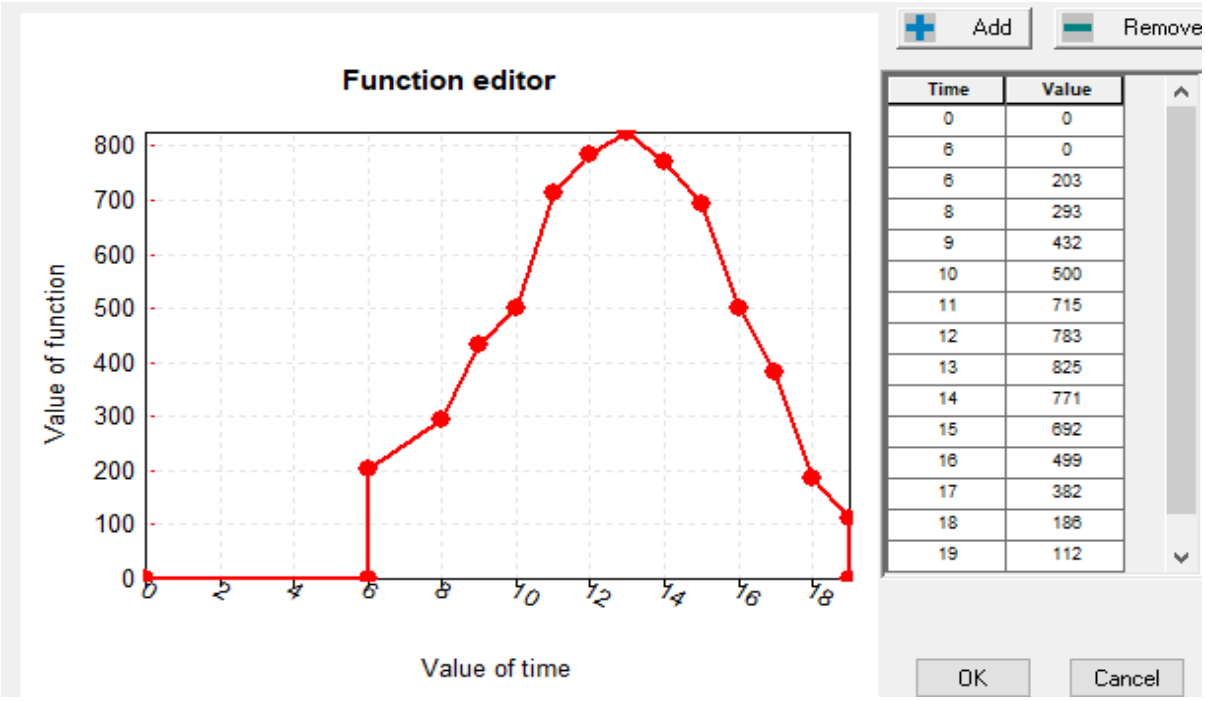

Figure 3. 3: Measured irradiation changes in term of time.

3.2.3.3. Type 14e:

We enter the ambient and inlet temperature passing through the solar collector in function of time of the air by going to the same previous steps as for the radiation but we choose another type for that, type14e and this type has the same principle of work as type14th but the difference between them is that type14e is specialized to temperature degree only but the type14th is general, standard and accept any unit.

3.2.3.4. Type 3a:

In order to enter the input flow rate, there is a fan connected to the solar air collector, in order to give us a fixed value for the inlet flow that will pass through the solar collector. so, we chose the Type 3a that is appropriate type to play the fan role in the simulation process of our work because it has a set of parameters that correspond to the input that we took from a real fan and that it also allows to entry the inlet temperature data obtained from Type 14e by linking, to type 73 (considered a solar collector), appear in the following table (3.1).

Table 3. 2: Fit parameters and input of Type 3a

	Name	Unit
Parameters	Maximum flow rate	kg/hr
	Maximum power	kJ/hr
Input	Inlet fluid temperature	°C

And In order for the fan to work regularly over time, we have used Type 14h, where we have entered the value 0 for the hours that the fan stops reacting and the value 1 for the hours that the experimental operation was made as shown in the flowing figure (3.3).

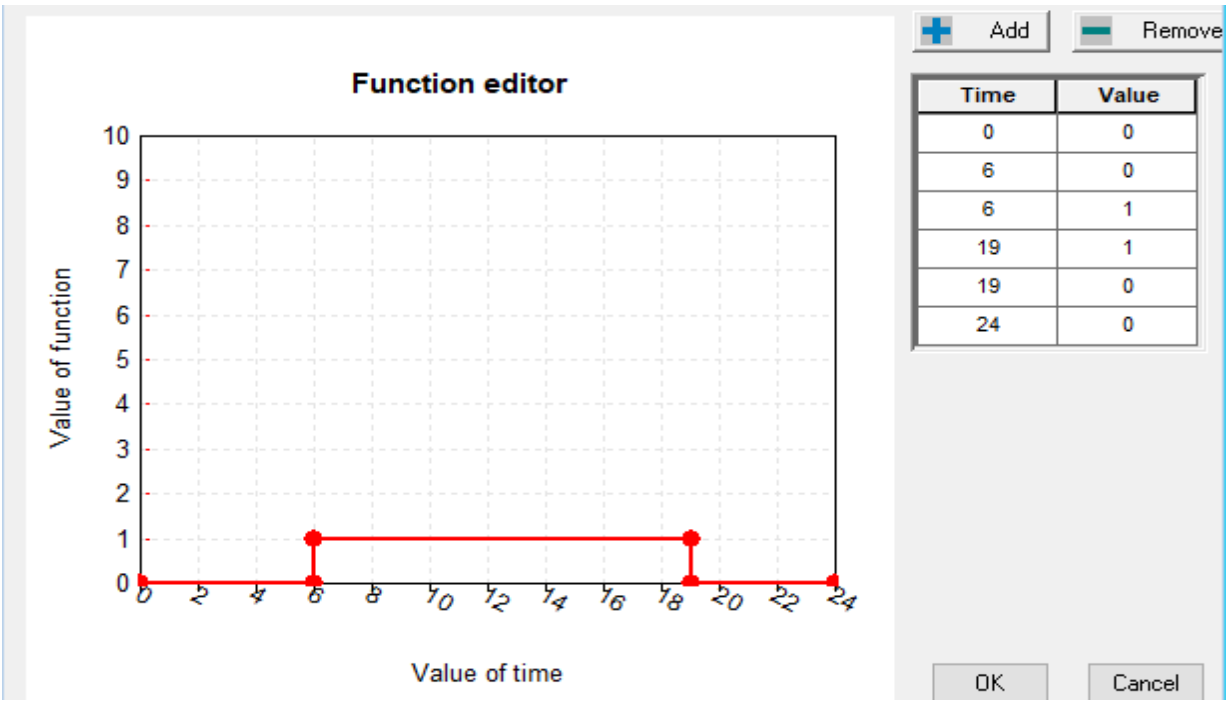

Figure 3.4: The reacting of Fan in function of time.

3.2.3.5. Type 65a

is a printing tool for the results that the TRNSYS program outputs from the simulation on the Data.txt.

3.3.Simulation methodology:

After we finished the comparison with experimental results and make sure of the validity of type 73 and the results obtained. We moved on to the next step which is the Simulation which differ from the Validation process where the design inputs depend on the results of our own Optimisation whit STSTGRAPHICS software to improve and increase the outlet temperature of the solar collector , and at this process we use the same TRNSYS software types that we have mentioned before but differ only in how to enter weather information where we use current and local weather information so we replace the Type 14h and Type 14e with Type109-TMY2 and this is shown in Figure (3.5), and that can be summarized as represented the figure (3.6).

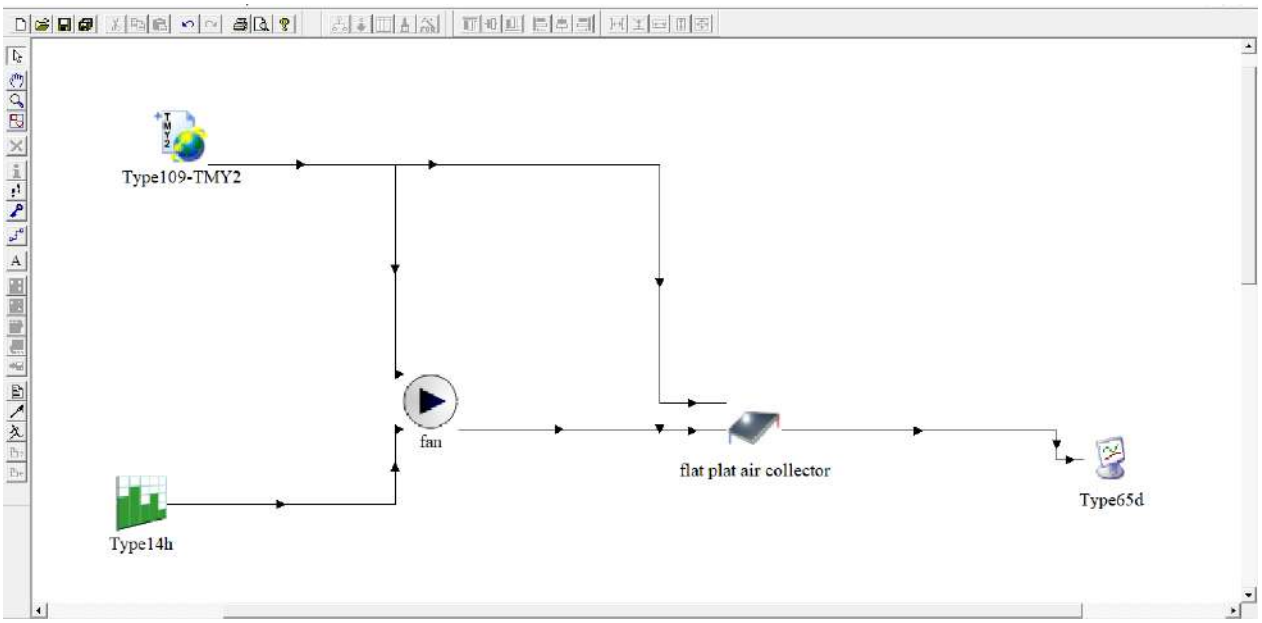

Figure 3.5: TRNSYS simulation studio

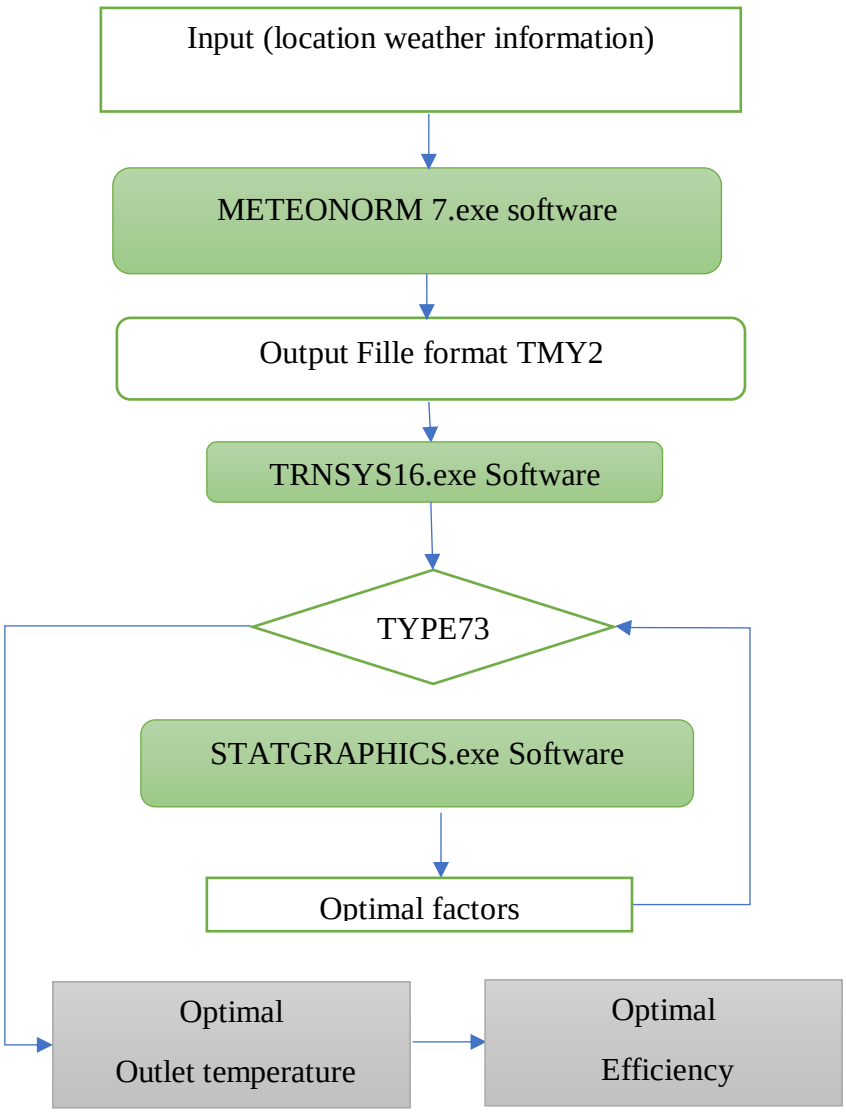

Figure 3.6: Simulation algorithm methodology

3.3.1. Fit types for simulation:

3.3.1.1. Type 109-TMY2:

Is the type of weather data, that allows us to input all the information about weather in the region of OUARGLA , In order to subdue the collector on climatic conditions we chose a particular set of outputs that match the input Type 73 as shown table (3.3) and figure (3.5), terms of ambient temperature, Total radiation on horizontal, Sky diffuse radiation on horizontal, Total radiation on

tited surface, Sky diffuse radiation on tited surface, Angle of incidence for tited surface, Slope of tited surface. And this type takes his information from METEONORM software, is a special software to extract all the weather information for the region.

Remarque: we adopted the 2017 date because the program 2 does not contain weather information for all months of the year 2018, considering that our puppies in the winter only while we need weather information in other chapters and selected weather information dated 2017 because he's closer to the current year.

Table 3.3: The Type 109-TMY2 fit output for Type 73

Nr	Name	Unit
1	Ambient temperature	℃
2	Total radiation on horizontal	$kJ/hr.m^2$
3	Sky diffuse radiation on horizontal	$kJ/hr.m^2$
4	Total radiation on tited surface	$kJ/hr.m^2$
5	Sky diffuse radiation on tited surface	$kJ/hr.m^2$
6	Angle of incidence for tited surface	degrees
7	Slope of tited surface	degrees

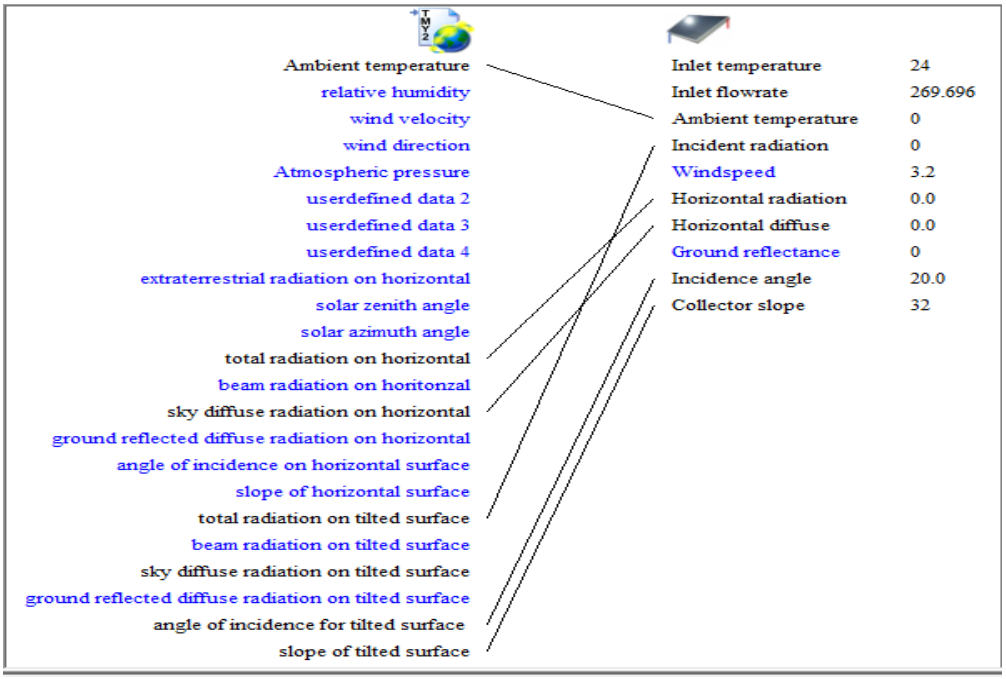

Figure 3.7: The link between Type 109-TMY2 outputs and Type 73 inputs

3.4. Optimization:

At this part of the study, our goal is to optimize the design of the solar collector in order to produce a maximum outlet temperature and efficiency, so we have adopted the design of experiments method that we have explained before in (chapter 02), we use for that, the STATGRAPHICS software which helps us quickly and effectively to accomplish our design of experiments, the DOE wizard in STATGRAPHICS, guides the user through twelve important steps.

3.4.1. Step 1: Define responses:

This step allows us to define our responses, in our case we have just the outlet temperature and we we've chosen these next options as shown in table (3.4).

We have chosen the response levels as shown in the following table (3.4), taking into account the reasonable values that the solar collector may reach during the winter period.

Table 3.4: Define response 'outlet temperature and efficiency'

Name	Units	Analyze	Goal	Target	Impact	Sensitivity	Low	High
outlet temperature	C	Mean	Maximize		3	High	40	80
efficiency		Mean	Maximize		3	High	0.2	0.4

- **Analyze** – the statistic to be analyzed. This setting is only relevant if you will be collecting multiple samples during each run, or if you create a robust parameter design with crossed factors;
- **Mean** – creates a model for the mean response. If Y_{ij} equals the measurement obtained from the i-th sample collected during the j-th run and letting m be the number of samples collected during that run, then the mean is calculated from;

$$\bar{Y}j = \frac{\sum_{i=1}^{m} Yij}{m} \qquad (3.2)$$

- **Goal**- The goal of the experiment is to maximize the outlet temperature;
- **Impact** – a number between 1.0 and 5.0 that describes the relative importance of each response. Sensitivity – how important it is to be close to the desired goal. This affects the shape of the desirability functions created during response optimization. [34]

3.4.2. Step 2: Define experimental factors

This step allows us to define our experimental factors that will be varied during the experiment.

And we've added the experimental controlled factors that effected on the outlet temperature and efficiency of the collector which chowed in flowing table (3.5)

Table 3.5: Defined controllable factors.

Name	Units	Type	Role	Low	High
A: Area	m^2	Continuous	Controllable	1.5	2.5
B: Absorptance of absorber plate	[-]	Categorical	Controllable	0.94	0.95
C: Index of refraction of cover	[-]	Categorical	Controllable	1.49	1.526
D: Extinction coeff. thickness prod	[-]	Continuous	Controllable	0.096	0.16
E: Inlet flow rate	kg/hr	Continuous	Controllable	35	55

3.4.3. Step 3: Select the experimental design

The third step in creating an experiment is to select an experimental design. This step allows us to specify the type of experiment that we want to work with, and in our case, we select screening-half-fraction design in order to reduce the number of experiments from 32 to 16 experiments, just because in our case, they give us the same results of factorial design, so there's no need to do all the experiments, which is the purpose of the half fraction design.

3.4.4. Step 4: Specify the initial model to be fit to the experimental results

This step allows us to specify the fitting model, and the typical model for screening is the 2-factor interactions model.

3.4.5. Step 5: Select an optimal subset of the runs (optional)

After the software gives us the number of experiments that can be done, this step 5 Allows us to determine how many experiments we see fit, we chose 16 experiments (16 runs selected).

And we complete all the experiments proposed by the STATGRAPHICS software and introduce the results (response) Represented the outlet temperature and efficiency in the "Databook" window figure (3.9).

	BLOCK	Collector area	Absorptance of absorber plate	Index of refraction of cover	Extinction coeff. thickness prod	Inlet flow rate	outlet temperature	efficiency
		m^2	-	-	-	Kg/hr	c	%
1	1	1	High	High	-1	-1	44.85	0.24
2	1	-1	Low	High	-1	-1	35.54	0.26
3	1	-1	High	High	1	-1	34.52	0.25
4	1	1	Low	High	1	-1	42.83	0.22
5	1	1	Low	High	-1	1	35.83	0.25
6	1	1	High	Low	-1	1	36.16	0.25
7	1	1	Low	Low	1	1	34.75	0.23
8	1	1	High	Low	1	-1	43.27	0.22
9	1	-1	Low	High	1	1	28.42	0.25
10	1	1	High	High	1	1	34.76	0.23
11	1	-1	Low	Low	1	-1	34.5	0.25
12	1	-1	High	Low	-1	-1	35.84	0.25
13	1	1	Low	Low	-1	-1	44.84	0.24
14	1	-1	Low	Low	-1	1	29.3	0.27
15	1	-1	High	High	-1	1	29.31	0.27
16	1	-1	High	Low	1	1	28.61	0.26

Figure 3.8: Databook window

3.4.6. Step 6: Evaluate design

This step generates a number of deferent options numerical and graphical summaries of the properties of selected design, that can use to know if the design is good in particular the predictive variance where should be relatively constant for the experiment region. The most Important options to have a good evaluation of the model in this step is the Leverage and prediction variance plot.

3.4.7. Step 7: Save design

In this step we save all the work we've done before and the results obtained as well, in an XML file whit the extension. sgx.

3.4.8. Phase 2: Analyzing the results

After we've creating our experiment we are going to move to analyzing the results

Step 8: Analyze data

This is done through the statistical models are constructed each response, keeping in mind the principle of "parsimony"

3.4.9. Step 9: Optimize the responses

In order to find a combination of the experimental factors that provides a good result for multiple response variables, the DOE Wizard uses the concept of desirability functions. [34]

"Desirability" is measured on a scale of 0 to 1 whit 1 being the most desirable.

When several responses suggest different optimal operating conditions, a balance between those responses is achieved using desirability functions.

3.4.10. Step 10: Save the results

this Step 10 allows us to save our results in a StatFolio

3.4.11. Step 11: Augment design

We don’t need to augment the design if we see the design are fairly clear.

3.4.12. Step 12: Extrapolate model

This step allows us to use the statistical model to predict settings of the factors outside the experimental region that might produce even better results.

3.5. Conclusion:

Through what we have done in this chapter we can sum it up that we have taken the three steps that are the structure on which our entire study was built, beginning validation, optimisation and then the numerical simulation using optimum factors, and we used two software that underpinned our study, and the first is a statistical software which is the "STATGRAPHICS software" that was used for the design of experiments to optimise the outlet temperature and efficiency of the solar collector, and the second one is a numerical simulation software "TRNSYS software" used to simulate the solar collector so we used in our study a systematic coupling between the two software, that gave us the possibility of testing and presenting the results in a very fast and efficient and that it contributed to reduce the proportion of error when compared to the experimental results.

.

Chapter 04:

Simulation and optimization of the solar air collector

4.1. Introduction:

In this chapter, we will present and discuss the results of the optimisation and the numerical simulation conducted in our study. Decision procedures and presentation of results based on the following three components:

a- Validation: This part of the study will allow us to validate the numerical results Taken from the simulation using TRNSYS software by comparison with the experimental measurements data available. Validation of the adopted numerical model using experimental results on an indirect solar dryer designed and realized in the Laboratory of Development of new and renewable energies in arid zones (LENREZA, Univ. Ouargla, Algeria).

b- Optimization: of the outlet temperature and efficiency of collector using the STATGRAPHICS Software basing on the Design of experiments method in the season of winter, 2th December 2017.

c- Simulation: numerical simulation based on the results presented by the optimisation and comparing it whit other work done before.

4.2. Validation:

Typical days were chosen in (May and June), 23-24-25/05/2011 and 06/06/2011.

In order to allow logical comparison, we conducted a simulation test to raise the point values of the temperature in the center of the air slide coming out of the sensor.

These values, for regular time intervals, were compared with the experimentally measured values for the same time intervals. All these simulated and calculated values are shown on the figures (4.1), (4.2), (4.3), (4.4). It can be observed, taking into account the studied phenomenon that the calculated and measured values are in good coherence with a maximum deviation of almost 6°C. This discrepancy can be explained by the difference between the actual climatic conditions (fluctuations in solar radiation and the wind velocity in the daytime) and those used by the calculation software, based on a typical regular evolution.

Table 4.1: The boundary condition of the May, 23th 2011[43].

Collector area=2.208 m^2

Type of Absorber use it =copper

Type of glass =Plexiglas

Thickness of glaze =5mm

Velocity=3.2 m/s

Air stream=7.5cm

Time	I_T (W/m^2)	V (m/s)	T_{amb} (°C)
7h	260	3,1	22,6
8 h	380	3,2	23,4
9 h	491	3,2	24,5
10 h	608	3,2	25,9
11 h	705	3,2	27,6
12 h	760	3,2	28,6
13 h	789	3,2	30,2
14 h	772	3,2	30,3
15 h	715	3,2	30,9
16 h	636	3,2	31,0
17 h	133	3,2	30,1
18 h	226	3,2	29,3
19 h		3,2	28

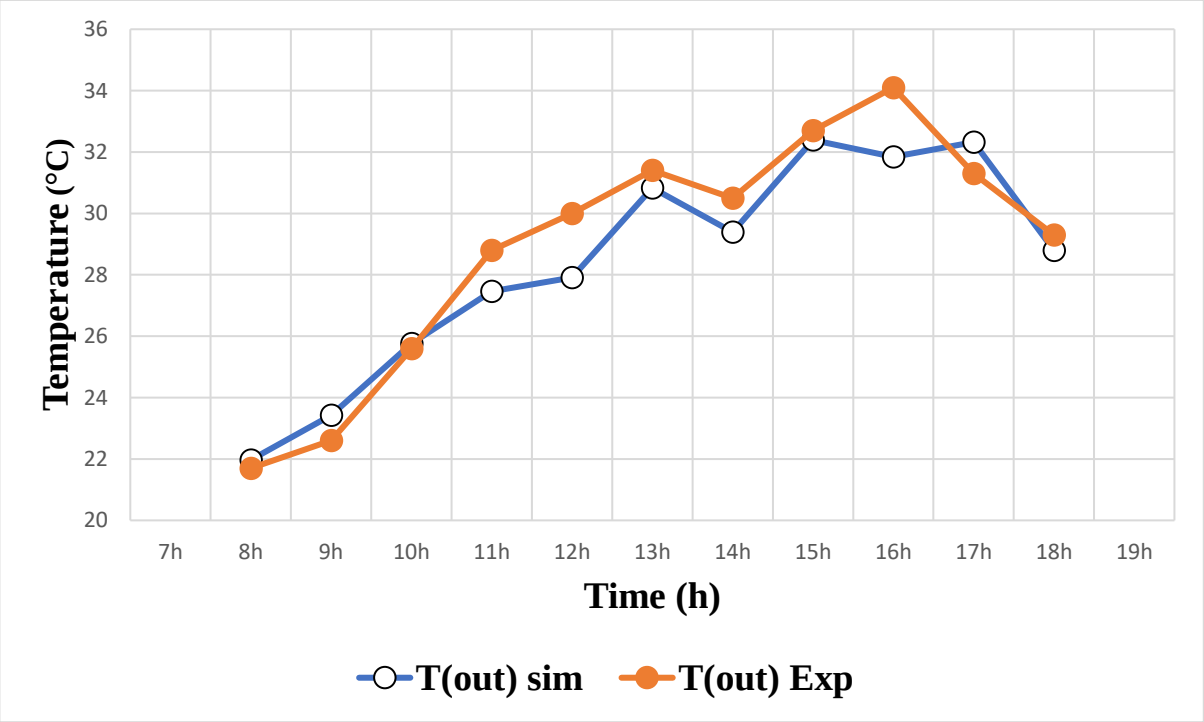

Figure 4.1: Simulated and experimental **outlet temperature** values on May, 23th 2011

Table 4.2: The boundary condition of the May, 24th 2011[43].

Collector area=2.208 m^2

Type of Absorber use it =copper

Type of glass =Plexiglas

Thickness of glaze =5mm

Velocity=3.2 m/s

Air stream=7cm

Time	I_T(W/m^2)	V (m/s)	T_{amb} (°C)
7 h	203	3,2	22,4
8 h	293	3,2	23,4
9 h	432	3,2	24,8
10 h	432	3,2	26,7
11 h	715	3,2	28,3
12 h	783	3,2	30,4
13 h	825	3,2	31,5
14 h	771	3,2	32,4
15 h	692	3,2	33,1
16 h	499	3,2	31,6
17 h	382	3,2	31,1
18 h	186	3,2	30
19 h	112	3,2	29,2

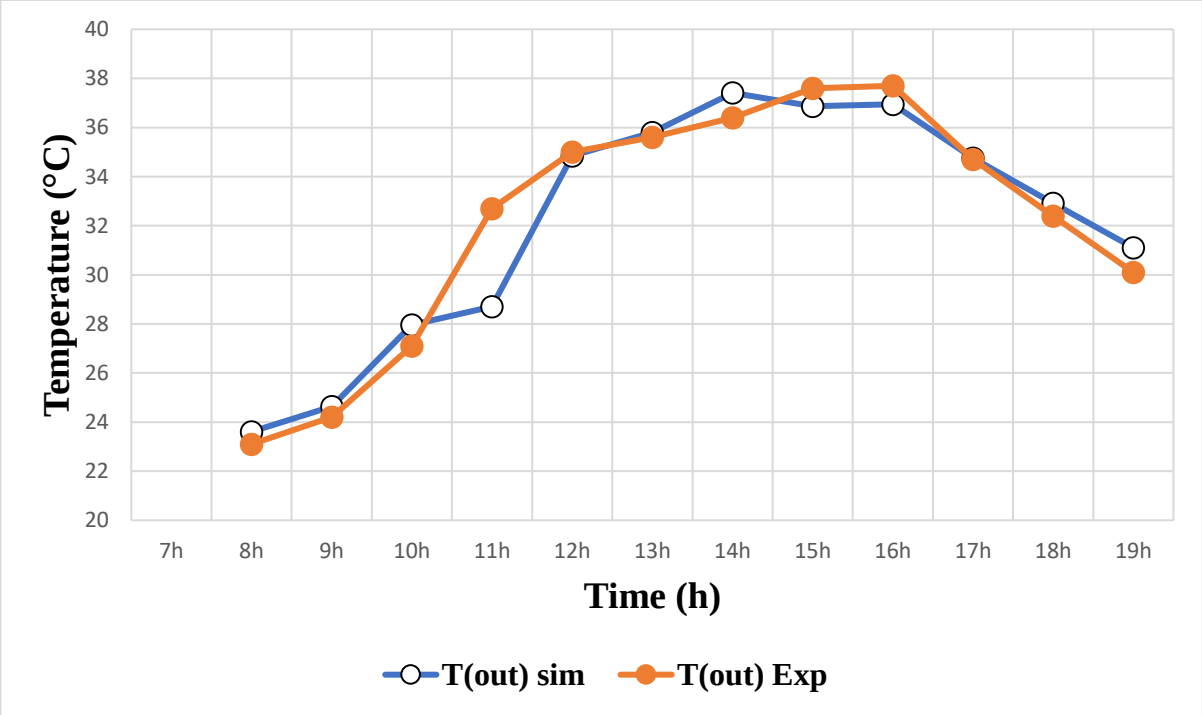

Figure 4.2: Simulated and experimental **outlet temperature** values on May, 24th 2011

Table 4.3: The boundary condition of the May, 25th 2011[43].

	Time	I_T (W/m^2)	V (m/s)	T_{amb}(°C)
Collector area=2.208 m^2	7 h30	495	3,1	32,6
Type of Absorber use it =copper	8 h	518	3,2	24,4
Type of glass =Plexiglas	9 h	556	3,2	25,2
Thickness of glaze =4mm	10 h	525	3,2	27,5
Velocity=3.2 m/s	11 h	560	3,2	28,9
Air stream=7cm	12 h	412	3,2	30,3
	13 h	496	3,2	30,8
	14 h	615	3,2	32,0
	15 h	667	3,2	32,8
	16 h	520	3,2	31,5
	17 h	732	3,2	31,4
	18 h	419	3,2	30,6
	18h30	345	3,2	30,1

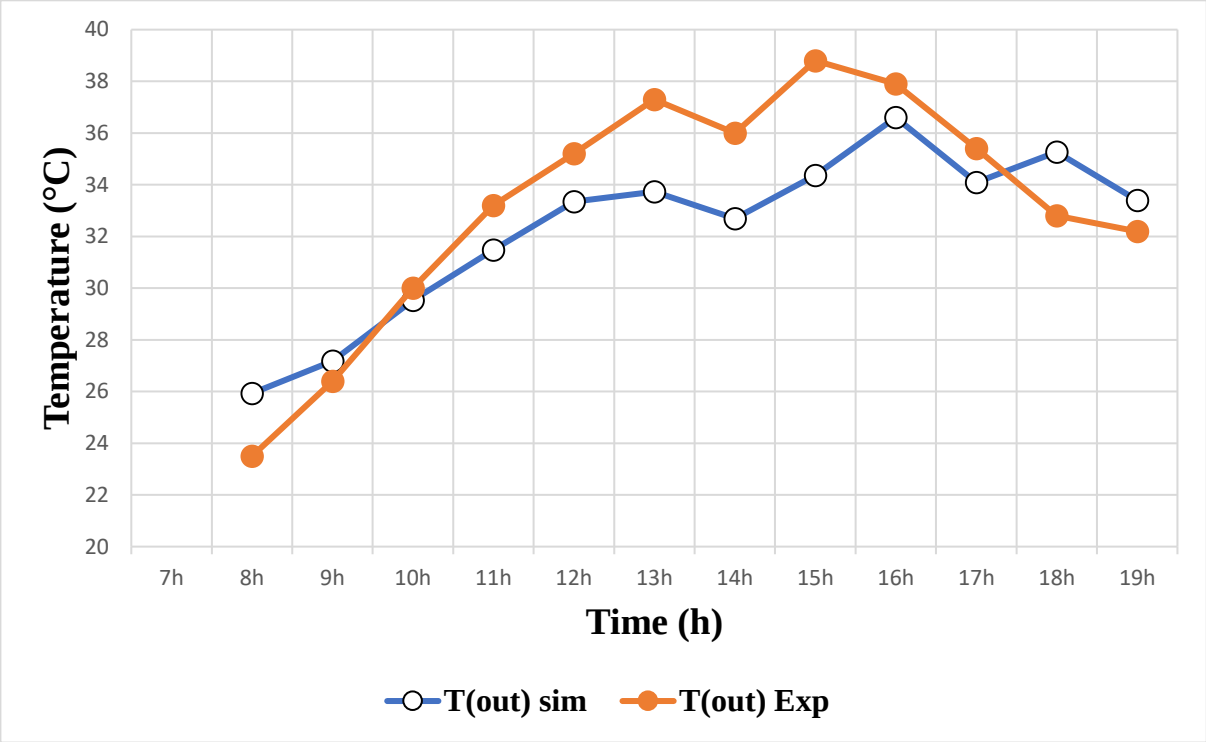

Figure 4.3: Simulated and experimental **outlet temperature** values on May, 25th 2011

Table 4.4: The boundary condition of the May, 23th 2011[43].

Collector area=2.208 m^2

Type of Absorber use it = Iron noxydable

Type of glass = glaze

Thickness of glaze =5mm

Velocity=3.2 m/s

Air stream=7cm

Time	I_T (W/m^2)	V (m/s)	T_{amb} (°C)
7 h	151	3.2	27,6
8 h	336	3.2	30,4
9 h	536	3.2	33,2
10 h	729	3.2	35,3
11 h	840	3.2	37,5
12 h	880	3.2	39,1
13 h	910	3.2	41,5
14 h	865	3.2	40,9
15 h	804	3.2	38,1
16 h	633	3.2	39,5
17 h	432	3.2	38,5
18 h	132	3.2	36,6
19 h	40	3.2	35,2

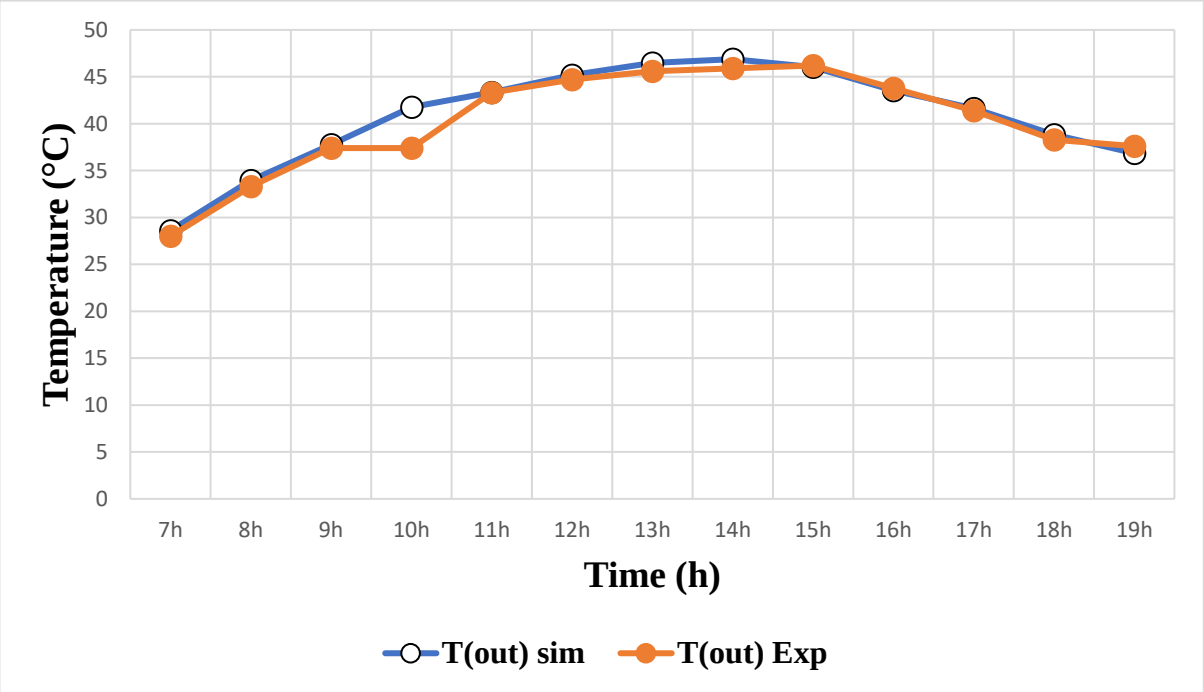

Figure 4.4: Simulated and experimental **outlet temperature** values on Jun, 23th 2011

4.3. Optimisation of the outlet temperature and efficiency:

4.3.1. Finding influential factors:

A first study was to develop a design of experiments to optimize the performance of the solar collector to be used as a component of an indirect solar dryer. Several parameters have been studied to determine the influence they had on the output temperature of the collector. These parameters are the measuring interval, continuous one's area of the collector and extinction coefficient-thickness prod and inlet flow rate, and categorical ones absorptance of absorber plate and Index of refraction of cover. For each of the continuous factors and categorical factors the levels of variation (low and high) -1 and +1 have been set and are shown in the table (4.5).

Table 4.5: Selection of factors studied and their levels of variation for the study conducted

	Continuous		
Factors	Variables	Level -1	Level +1
X_1	Collector area [m^2]	1.5	2.5
X_4	Extinction coefficient- thickness prod [-]	0.096	0.16
X_5	inlet flow rate [kg/hr]	35	55
	Categorical		
X_2	Absorptance of absorber plate [-]	0.94	0.95
X_3	Index of refraction of cover [-]	1.49	1.526

The experiment design that has been used is a half fraction design whose General construction was described in paragraph (chapter 02). Thus, we can see in the table (4.6) the experiments that have been carried out, having five factors at 2 levels. This represents therefore $\mathbf{2^{5-1} = 16}$ experiments as well as the measured responses. The response noted Y1outlet temperature and Y2 efficiency of the collector which determined whit the flowing equation (4.1):

$$\eta_{En} = \frac{Q_u}{A_p I_T} = \frac{\dot{m} C_P (T_{f,out} - T_{f,in})}{A_p I_T} \qquad (4.1)$$

Q_u= thermal energy, W

ṁ= mass flow rate, kg/hr

C_P= specific heat, $kJ/kg.K$

T= temperature, K

A_p= absorption area, m^2

I_T=Total radiation kJ$/hr\ m^2$

Table 4.6: Half fraction design $\mathbf{2^{5-1}}$with variables in coded X and natural values U as well Y as responses.

Runs	X1	X2	X3	X4	X5	U1	U2	U3	U4	U5	Y1	Y2
1	+1	+1	+1	-1	-1	2.5	0.95	1.526	0.096	35	44.85	0.24
2	-1	-1	+1	-1	-1	1.5	0.94	1.526	0.096	35	35.54	0.26
3	-1	+1	+1	+1	-1	1.5	0.95	1.526	0.16	35	34.52	0.25
4	+1	-1	+1	+1	-1	2.5	0.94	1.526	0.16	35	42.83	0.22
5	+1	-1	+1	-1	+1	2.5	0.94	1.526	0.096	55	35.83	0.25
6	+1	+1	-1	-1	+1	2.5	0.95	1.49	0.096	55	36.16	0.25
7	+1	-1	-1	+1	+1	2.5	0.94	1.49	0.16	55	34.75	0.23
8	+1	+1	-1	+1	-1	2.5	0.95	1.49	0.16	35	43.27	0.22
9	-1	-1	+1	+1	+1	1.5	0.94	1.526	0.16	55	28.42	0.25
10	+1	+1	+1	+1	+1	2.5	0.95	1.526	0.16	55	34.76	0.23
11	-1	-1	-1	+1	-1	1.5	0.94	1.49	0.16	35	34.5	0.25
12	-1	+1	-1	-1	-1	1.5	0.95	1.49	0.096	35	35.84	0.25
13	+1	-1	-1	-1	-1	2.5	0.94	1.49	0.096	35	44.84	0.24
14	-1	-1	-1	-1	+1	1.5	0.94	1.49	0.096	55	29.3	0.27
15	-1	+1	+1	-1	+1	1.5	0.95	1.526	0.096	55	29.31	0.27
16	-1	+1	-1	+1	+1	1.5	0.95	1.49	0.16	55	28.61	0.26

4.3.2. Analysis:

4.3.2.1. Regression coefficients for outlet temperature:

From the values of the effects or coefficients shown in table (4.7), (4.8) the following mathematical models can be expressed for our response:

Table 4.7: Interactions and quadratic effects on the response **Y1**

Coefficient	Estimate
Constant	35.8331
A: Collector area	3.82813
B: Absorptance of absorber plate	0.081875
C: Index of refraction of cover	-0.07563
D: Extinctioncoeff. thickness prod	-0.62563
E: Inlet flow rate	-3.69062
AB	0.016875
AC	-0.01813
AD	-0.13313
AE	-0.59563
BC	0.020625
BD	0.000625
BE	-0.01438
CD	0.000625
CE	0.013125
DE	0.118125

Table 4.8: Interactions and quadratic effects on the response **Y2**

Coefficient	Estimate
Constant	0.24625
A: Collector area	-0.01125
B: Absorptance of absorber plate	0
C: Index of refraction of cover	0
D: Extinction coeff. thickness prod	-0.0075
E: Inlet flow rate	0.005
AB	0
AC	0
AD	-0.0025
AE	0
BC	0.00125
BD	0.00125
BE	0.00125
CD	-0.00125
CE	-0.00125
DE	-0.00125

This pane displays the regression equation which has been fitted to the data. The fit mathematical model for the response **Y1** is:

$$\begin{aligned} Y1 = {} & 35.8331 + 3.82813X_1 + 0.081875X_2 - 0.075625X_3 - 0.625625X_4 \\ & - 3.69062X_5 + 0.016875X_1X_2 - 0.018125X_1X_3 \\ & - 0.133125X_1X_4 - 0.595625X_1X_5 + 0.020625X_2X_3 \\ & + 0.000625X_2X_4 - 0.014375X_2X_5 + 0.000625X_3X_4 \\ & + 0.013125X_3X_5 + 0.118125X_4X_5 \end{aligned} \quad (4.2)$$

Mathematical model for the second response **Y2** is:

$$\begin{aligned} Y2 = {} & 0.24625 - 0.01125X_1 + 0.0X_2 + 0.0X_3 - 0.0075X_4 + 0.005X_5 \\ & + 0.0X_1X_2 + 0.0X_1X_3 - 0.0025X_1X_4 + 0.0X_1X_5 + 0.00125X_2X_3 \\ & + 0.00125X_2X_4 + 0.00125X_2X_5 - 0.00125X_3X_4 - 0.00125X_3X_5 \\ & - 0.00125X_4X_5 \end{aligned} \quad (4.3)$$

4.3.2.2. Pareto chart:

The Pareto chart in Figure 4.5 and 4.6 shows all of the parameter effects and their interactions in decreasing order of importance. The (+) sign indicates a positive contribution of the effect, while the (-) sign indicates a negative contribution [45].

In the case of outlet temperature, there are main effects (A: collector area, E: Inlet flow rate, and D: Extinction coeff. thickness prod, B: Absorptance of absorber plate, C: Index of refraction of cover) and three significant interactions (AE, AD and DE).

And in the case of efficiency we have only three main effects (A: collector area, E: Inlet flow rate and D: Extinction coeff. thickness prod) and seven significant interactions (AD, DE, CE, CD, BE, BD, BC).

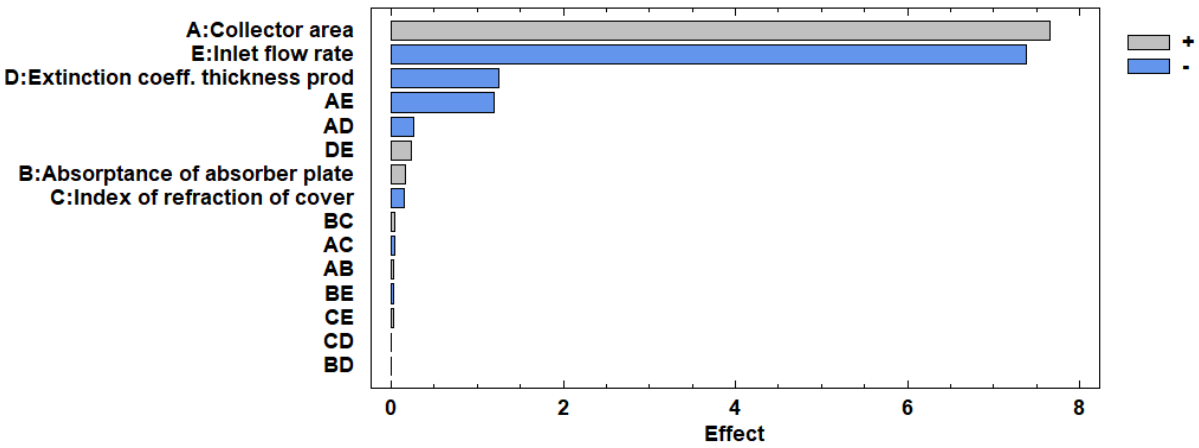

Figure 4.5: Standardized Pareto chart for **outlet temperature**

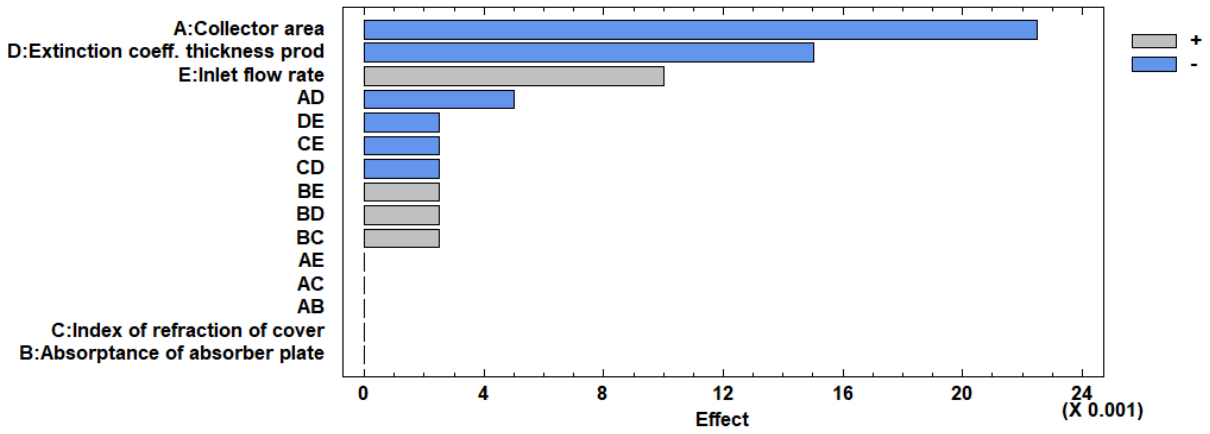

Figure 4.6: Standardized Pareto chart for **efficiency**

The values given in Figure 4.5 indicate that all of those interactions (BC, CA, AB, BE, CE, CD, BD) are negligible. Those interactions may therefore be eliminated from the model. This adjustment did not affect model adequacy, and for figure 4.6 we have two factor and three interactions can be neglected, which are (C, B, AE, AC, AB).

The fitted models of outlet temperature and efficiency after removing the insignificant effects is given in equation (4.4) and equation (4.5).

$$Y1 = 35.83 + 3.83X_1 + 0.08X_2 - 0.076X_3 - 0.63X_4 - 3.69X_5 - 0.13X_1X_4 - 0.60X_1X_5 + 0.12X_4X_5 \quad (4.4)$$

$$Y2 = 0.24625 - 0.01125X_1 - 0.0075X_4 + 0.005X_5 - 0.0025X_1X_4 + 0.00125X_2X_3 + 0.00125X_2X_4 + 0.00125X_2X_5 - 0.00125X_3X_4 - 0.00125X_3X_5 - 0.00125X_4X_5 \quad (4.5)$$

Figure 4.7 shows a vertical blue line to determine which effects are statistically significant. The length of each bar is proportional to the value of the statistic calculated

for the associated effect. Any bars beyond the vertical line are statistically significant at the selected level of significance.

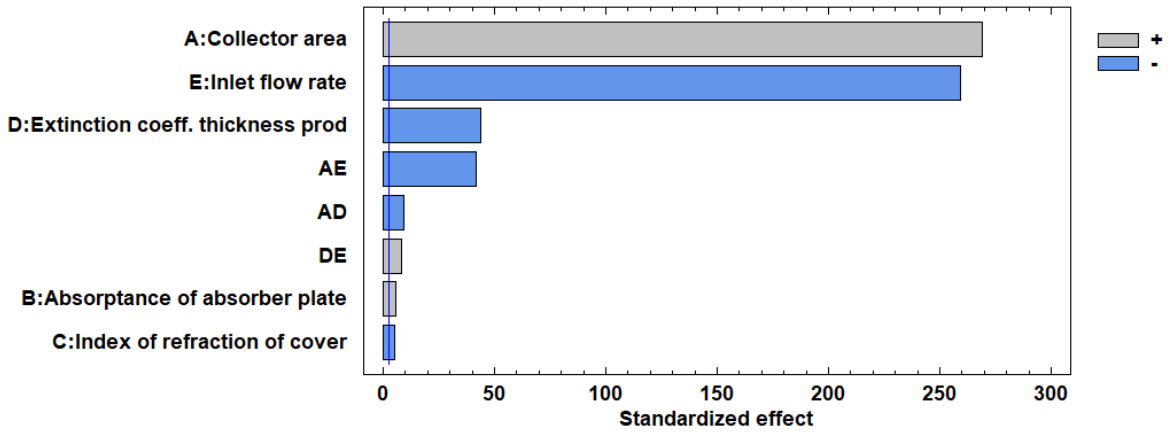

Figure 4.7: Standardized pareto chart for **outlet temperature** after excluding non-influence factors.

In figure (4.8) shows us the final form of pareto chart after excluding the non-effective factors where the valueof the estimated coefficient was 0.0 as shown in table (4.8).

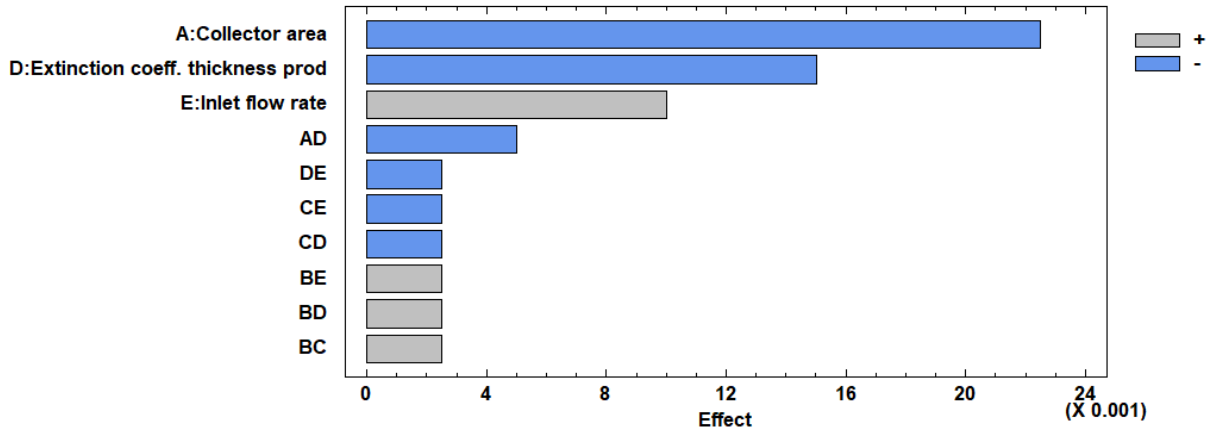

Figure 4.8: Standardized pareto chart for **efficiency** after excluding non-influence factors

4.3.2.3. Main effects plot:

The main effects plot depicted in Figure (4.9) and (4.10) shows the estimated change in outlet temperature and efficiency of the plat flat solar air collect, when each of the factors is shifted from its lowest level (-1) to its highest level (+1), with all other factors held constant at (0).

In figure (4.9), The plot reveals that the outlet temperature of the flat plat solar air collector decreases as increases (Inlet flow rate and Extinction coefficient- thickness prod). This can be explained by the fact that the increased inlet flow rate has a low heat transfer process between the absorbent plate and the air (convection), and with the increase in glass thickness reduces the rate of solar radiation entering the solar collector. In addition, this graph shows that two factors, namely collector area (left) and Inlet flow rate (right) have a greater effect than absorptance of absorber plate, Index of refraction of cover and Extinction coefficient- thickness prod (middle curve). The plot of each of these factors had an effect at the range 0 to +1 on our response, (collector area effect is equal =3.83℃, absorptance of absorber plate = 0.08℃), (inlet flow rate = 3.69℃, Extinction coefficient thickness prod = 0.63℃ and Index of refraction of cover = 0.076℃) which can be justified by the equation (4.4)

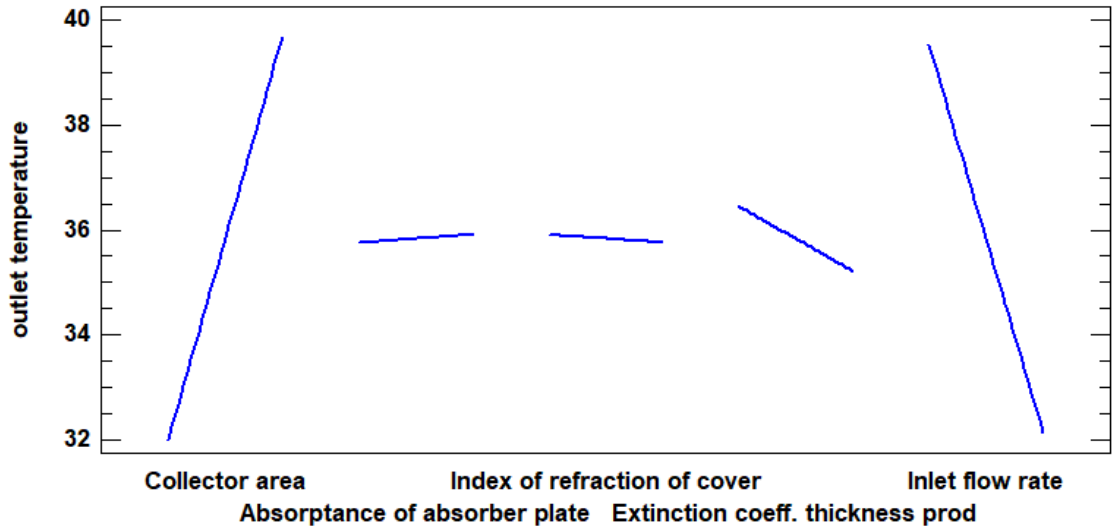

Figure 4.9: Main effects plot for **outlet temperature**

In figure (4.10), The plot reveals that the efficiency of the flat plat solar air collector decreases as increases (collector area and Extinction coefficient- thickness prod). This can be explained mathematically, when we refer to the equation for the efficiency of the solar collector we find that the area in the (denominator) and the temperature in the (numerator), the greater the amount of collector area (denominator) the value of the efficiency increases, and as for the thickness of the glass the smaller the greater the temperature (numerator) the efficiency increases, and in contrast, the value of effectiveness increases as the flow is increased as a (denominator).

The plot of each of these factors had an effect at the range 0 to +1 on our response, (collector area effect is equal =0.01125%,Extinction coefficient thickness prod = 0.0075% and the Inlet flow rate = 0.005%,which can be justified by the equation (4.5).

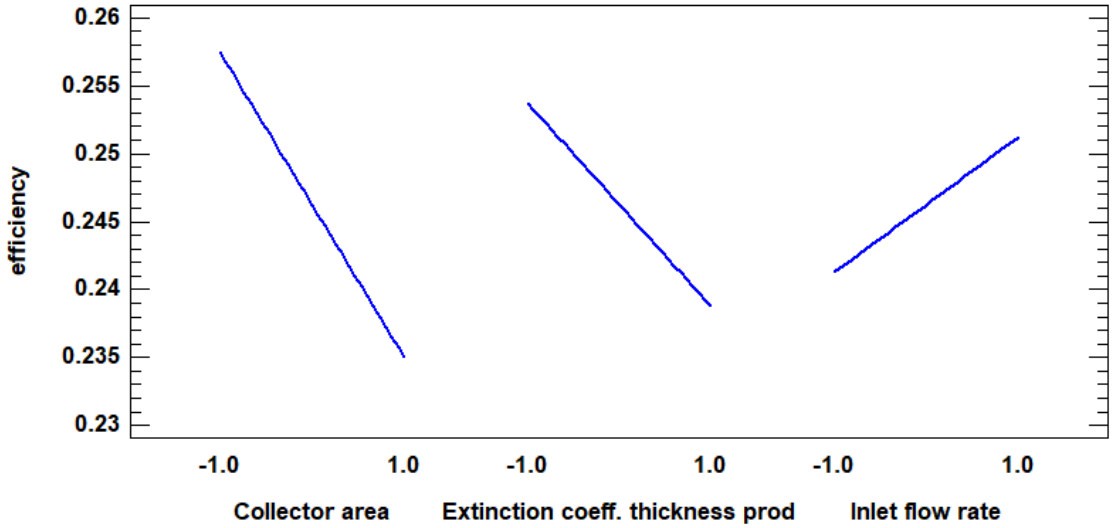

Figure 4.10: Main effects plot for **efficiency**

4.3.2.4. Interaction plot for outlet temperature and efficiency of plat flat solar collector:

In order to determine whether the process parameters are interacting or not, one can use a simple but powerful graphical tool called interaction plot. If the lines in the interaction plot are parallel, there is no interaction between the process parameters. This implies that the change in the outlet temperature from -1 to +1 levels of a factor does not depend on the level of the other factor. On the other hand, if the lines are non-parallel, an interaction exists between the factors. The greater the degree of departure from being parallel, the stronger the interaction effect.

Figure (4.11) illustrates the interaction plot for outlet temperature between 'A' (Area), 'D' (Extinction coeff. thickness prod) and 'E' (Inlet flow rate).

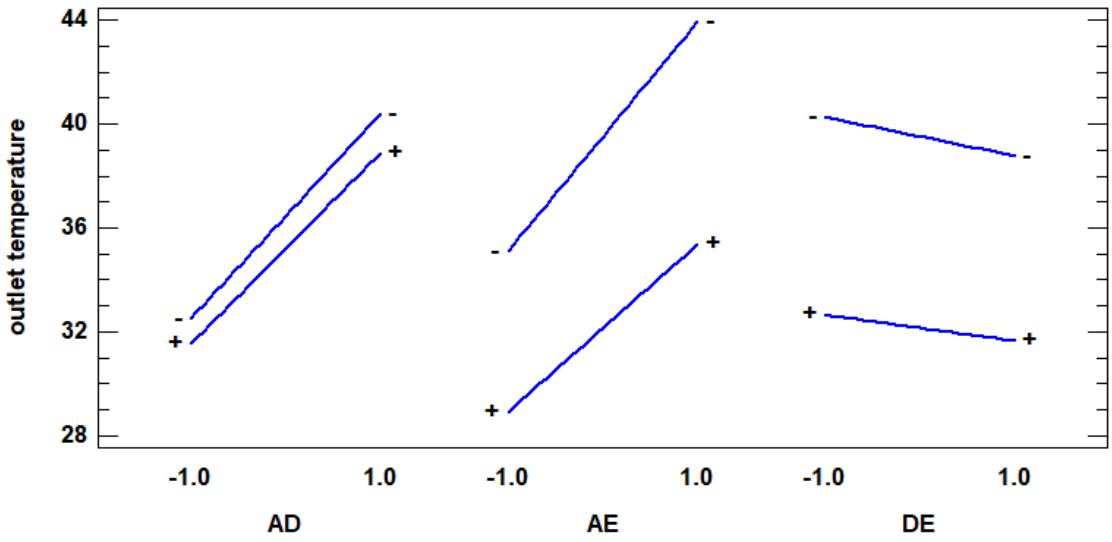

Figure 4.11: Interaction plot for **outlet temperature**.

- **The interaction (AD) plot between 'Area' and 'Extinction coeff. thickness prod'**

This plot shows that the effect of Area on outlet temperature at two different levels of (Extinction coefficient. Thickness) is determined as$(38.9 - 31.5)/2 = 3.65℃$for the (+1) and $(40.4 - 32.5)/2 = 3.95℃$ for the (-1). And the interaction is determined as $(31.5 - 38.8 - 32.5 + 40.4)/4 = 0.13℃$ This implies that there is an interaction between these two process parameters. This signifies that the effect of collector area is higher when the Extinction coefficient. Thickness is at the low level. When the collector area is $1.5m^2$, the effect of Extinction coefficient. Thickness is at $0.5℃$, when the collector area is at $2.5m^2$, the effect ofExtinction coefficient. Thickness is at $0.8℃$, this too signifies that the effect of Extinction coefficient. Thickness is higher when the collector area is at high level. The defect rate in (outlet temperature) is maximum$40.5℃$ when the Area is at +1 level and (Extinction coefficient. Thickness) at -1 level. This can be explained thermodynamically, as the area of the solar collector increases as the heat transfer area increases, so the temperature of the collector rises, and the thickness of the cover glass, the thicker the thickness, the more the permeability of the glass to the solar radiation.

- **The interaction (AE) plot between Area and inlet flow rate**

Shows the effect of Area on outlet temperature at two different levels of inlet flow rate is$4.5℃$ for (-1) and $3.35℃$ for (+1) this signifies that the effect of collector area is higher when the inlet flow rate is at low level, and the interaction between the two factors is determined as

$(-3.35-(-4.5))/2 =$ 0.6℃ and this implies that there is an interaction between these two process parameters. When the collector area is $1.5m^2$, the effect of Inlet flow rate is at 3.05℃ , when the collector area is at $2.5m^2$, the effect of Inlet flow rate is at 4.5℃, this too signifies that the effect of Inlet flow rate is more important when the collector area is at high level. The defect rate in (outlet temperature) is maximum44℃ when the collector area is at +1 level and Inlet flow rate at -1 level. And it's realistic because the more the flow, the lower the heat transfer from the absorber plate to the air.

- **The interaction (DE) plot between 'Extinction coeff. thickness prod' and 'Inlet flow rate'**

shows that the effect of 'Extinction coeff. thickness prod' on outlet temperature at two different levels of Inlet flow rate is 0.35℃for (+1) and 0.59℃ for (-1), this signifies that the effect of 'Extinction coeff. thickness prod' is higher when the inlet flow rate is at low level. The interaction between the two factors is determined as $(-0.35-(-0.59))/2 = 0.12$℃. This implies that there is an interaction between these two process parameters. When the 'Extinction coeff. thickness prod is 0.096, the effect of Inlet flow rate is at 3.75℃ , when the 'Extinction coeff. thickness prodis at 0.16, the effect of Inlet flow rate is at 2.75℃.This signifies that the effect of Inlet flow rate is more important when the 'Extinction coeff. thickness prodis at low level. The defect rate in (outlet temperature) is maximum 41 when the Extinction coeff. thickness is at -1 level and Inlet flow rate at -1 level.

In the next figure (4.12) illustrates the interaction plot for efficiency between 'A' (Collector area), 'D' (Extinction coeff. thickness prod), 'E' (Inlet flow rate), 'C' (Index of refraction of cover), 'B' (Absorptance of absorber plate).

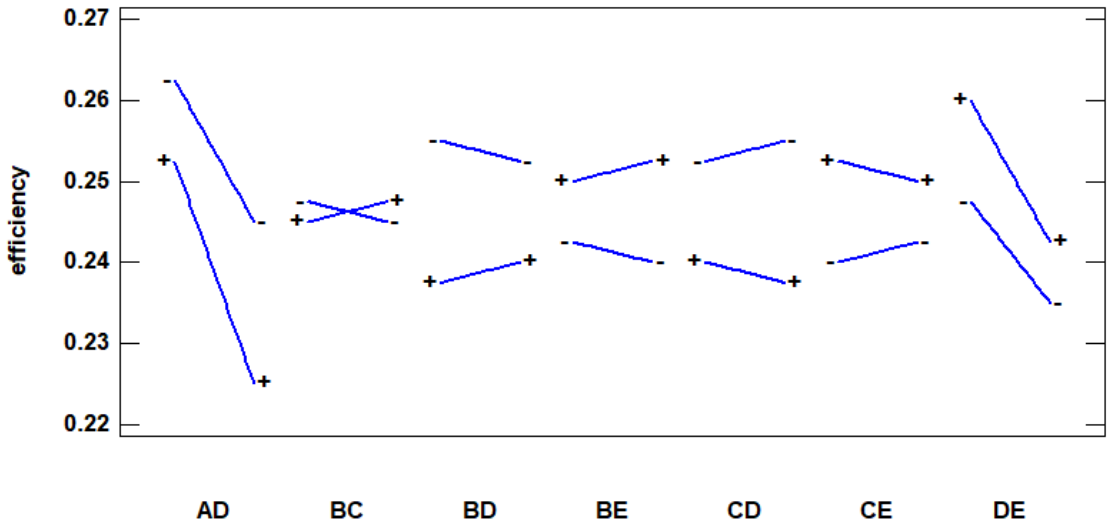

Figure 4.12: Interaction plot for **efficiency**

- **The interaction (AD) between 'collector area' and 'Extinction coeff. Thickness prod '**

This plot shows that the effect of collector area on efficiency at two levels of 'Extinction coeff. Thickness prod, (+1) and (-1) are respectively0.014% and 0.009%, this signifies that the effect of collector area is higher when the 'Extinction coeff. Thickness prod is at high level. The interaction between the two factors is determined as $(-0.014-(-0.009))/2 = -0.0025\%$, This implies that there is an interaction between these two process parameters. When the collector area is $1.5m^2$, the effect of 'Extinction coeff. Thickness prod' is at 0.005% , when the collector area is at $2.5m^2$, the effect of 'Extinction coeff. Thickness prod' is at 0.01%, this signifies that the effect of 'Extinction coeff. Thickness prod' is more important when the collector area is at high level. The defect rate in (efficiency) is maximum0.263% when the collector is at +1 level and 'Extinction coeff. Thickness prod' at -1 level.

- **The interaction (BC)between 'Absorptance of absorber plate' and 'Index of refraction of cover'**

this plot shows that the effect of Absorptance of absorber plate on efficiency at two levels of Index of refraction of cover (+1) and (-1) is not the same. This implies that there is an interaction between these two process parameters. When the Absorptance of absorber plate is 0.94 and 0.95 the effect of Index of refraction of cover is 0.0015%, this signifies that the effect of 'Index of refraction of cover' is the same when the collector area is at +1 and -1 level. the defect rate

in (efficiency) is maximum0.248% when the Absorptance of absorber plate is at -1 and +1 level and 'Index of refraction of cover at -1 and +1 level.

- **The interaction (BD) between 'Absorptance of absorber plate' and 'Extinction coeff. Thickness prod'**

This plot shows that the effect of Absorptance of absorber plate on efficiency at two levels of 'Extinction coeff. Thickness prod, (+1) and (-1) is not the same, this implies that there is an interaction between these two process parameters. When the Absorptance of absorber plate is 0.94, the effect of 'Extinction coeff. Thickness prod' is at 0.00925%, when the Absorptance of absorber plate is at 0.95, the effect of 'Extinction coeff. Thickness prod' is at 0.0065%, this signifies that the effect of 'Extinction coeff. Thickness prod' is more important when the Absorptance of absorber plate is at low level. The defect rate in (efficiency) is maximum0.256% when the Absorptance of absorber plate is at -1 level and 'Extinction coeff. Thickness prod' at -1 level. Shows the defect rate in (efficiency) is maximum0.255% when the 'Absorptance of absorber plate' is at -1 level and 'Extinction coeff. Thickness prod' at -1 level.

- **The interaction (BE) between 'Absorptance of absorber plate' and 'Inlet flow rate'**

This plot shows that the effect of Absorptance of absorber plate on efficiency at two levels of Inlet flow rate, (+1) and (-1) are respectively 0.0015% and 0.00125%, this signifies that the effect of Absorptance of absorber plate is higher when the Inlet flow rate is at high level. The interaction between the two factors is determined as $(-0.00125-(-0.0015))/2 = 0.00125\%$, This implies that there is an interaction between these two process parameters. When the Absorptance of absorber plate is 0.94, the effect of Inlet flow rate is at 0.003%, when the Absorptance of absorber plate is at 0.95, the effect of Inlet flow rate is at 0.00575%, this signifies that the effect of Inlet flow rate is more important when the Absorptance of absorber plate is at high level. The defect rate in (efficiency) is maximum 0.253% when the Absorptance of absorber plate is at +1 level and Inlet flow rate at +1 level.

- **The interaction (CD) plot between 'Index of refraction of cover' and 'Extinction coeff. thickness prod'**

This plot shows that the effect of 'Index of refraction of cover' on efficiency at two levels of 'Extinction coeff. Thickness prod', (+1) and (-1) is not the same, this implies that there is an interaction between these two process parameters. When the 'Index of refraction of cover' is

0.096, the effect of 'Extinction coeff. Thickness prod' is at 0.0055%, when the Absorptance of absorber plate is at 0.16, the effect of 'Extinction coeff. Thickness prod' is at 0.00925%, this signifies that the effect of 'Extinction coeff. Thickness prod' is higher when the 'Index of refraction of cover' is at high level. The defect rate in (efficiency) is maximum 0.256% when the 'Index of refraction of cover' is at +1 level and 'Extinction coeff. Thickness prod' at -1 level.

- **The interaction (CE) plot between 'Index of refraction of cover' and 'Inlet flow rate'**

This plot shows that the effect of 'Index of refraction of cover' on efficiency at two levels of Inlet flow rate, (+1) and (-1) is not the same, this implies that there is an interaction between these two process parameters. When the 'Index of refraction of cover' is 1.49,the effect of Inlet flow rate is at0.0065%, when the 'Index of refraction of cover' is at 1.526, the effect of Inlet flow rate is at 0.0035%, this signifies that the effect of Inlet flow rate is higher when the 'Index of refraction of cover' is at high level. The defect rate in (efficiency) is maximum 0.253% when the 'Index of refraction of cover' is at -1 level and Inlet flow rate at-1 level.

- **The interaction (CD) plot between 'Index of refraction of cover' and 'Extinction coeff. thickness Prod'**

This plot shows that the effect of 'Index of refraction of cover' on efficiency at two levels of 'Extinction coeff. thickness Prod', (+1) and (-1) are respectively 0.009% and 0.0065%, this signifies that the effect of 'Index of refraction of cover' is higher when the 'Extinction coeff. Thickness prod' is at high level. The interaction between the two factors is determined as $(-0.0065-(-0.009))/2 = -0.00125\%$, This implies that there is an interaction between these two process parameters. When the 'Index of refraction of cover' is 1.49, the effect of 'Extinction coeff. thickness Prod' is at 0.0065%, when the 'Index of refraction of cover' is at 1.526, the effect of 'Extinction coeff. thickness Prod' is at 0.004%, this signifies that the effect of 'Extinction coeff. Thickness prod' is higher when the 'Index of refraction of cover' is at low level. The defect rate in (efficiency) is maximum 0.261% when the 'Index of refraction of cover' is at -1 level and 'Extinction coeff. thickness Prod' at +1 level.

4.3.2.5. Response surface:

The surface plot displays a plot of the predicted response as a function of any two of the experimental factors, with the other factors held at selected values [36].

1- the figure (4.13) and figure (4.14) below shows respectively the outlet temperature as a function of Area and Inlet flow rate, and other factors are fixed on-1 and +1 level.

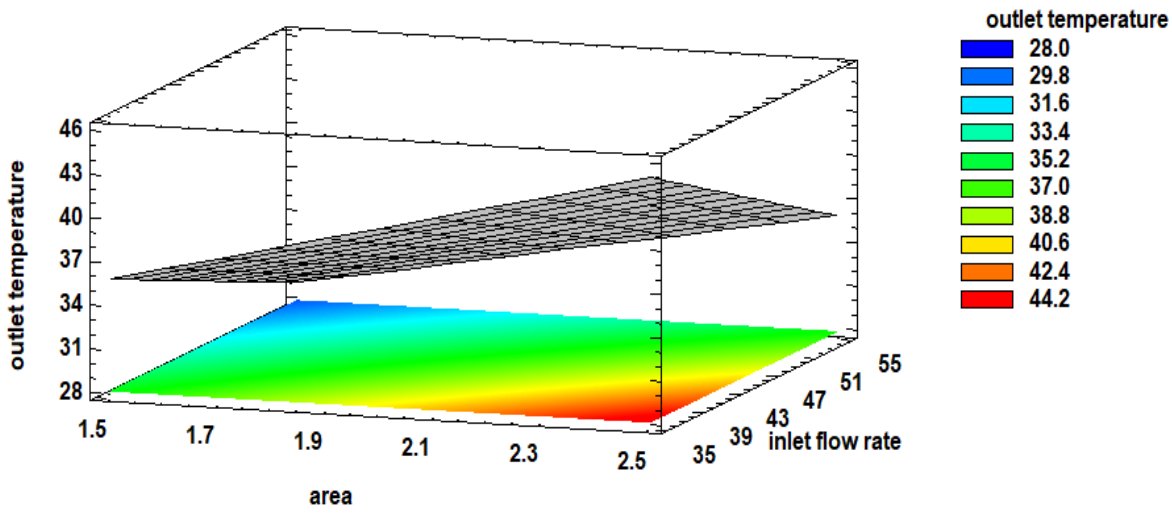

Figure 4.13: Estimated Response Surface con for the **Outlet Temperature** as function of Area and Inlet flow rate and other factors fixed on -1 level.

Note Through this figure, the temperature changes in the form of three zones in the contour below the surface which clearly shows us how the response surface changes, (Red, Green and blue zone), the temperature in the Red zone 44.2℃ in the range $[2-2.5]m^2$ of Area and $[35;47]$kg/hr of inlet flow rate, for the green zone the temperature is 38.8℃ in the range $[1.5-2.5]m^2$ and $[35-55]kg/hr$, And in the case of the blue zone the outlet temperature is 28℃ in the range $[1.5-2]m^2$ and $[43-55]kg/hr$.

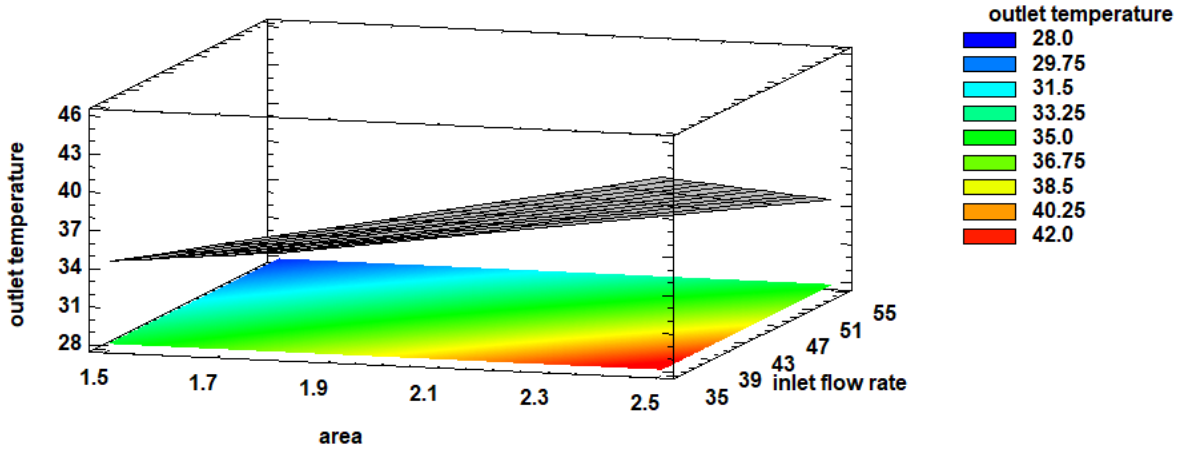

Figure 4.14: Estimated Response Surface for the **Outlet Temperature** as function of Area and Inlet flow rate and other factors fixed on +1 level.

Note Through this figure (4.14) the temperature in the Red zone is 42℃ in the range $[2-2.5]m^2$ of Area and $[35-45]$kg/hr of inlet flow rate, for the green zone the temperature is 36.75℃ inthe range $[1.5-2.5]m^2$ and $[35-55]kg/hr$, And in the case of the blue zone the outlet temperature is 28℃ in the range $[1.5-2]m^2$ and $[44-55]kg/hr$.

2- the figure (4.15) and figure (4.16) below shows respectively the outlet temperature as a function of Area and Extinction coeff. thickness, and other factors are fixed on -1 and +1 level.

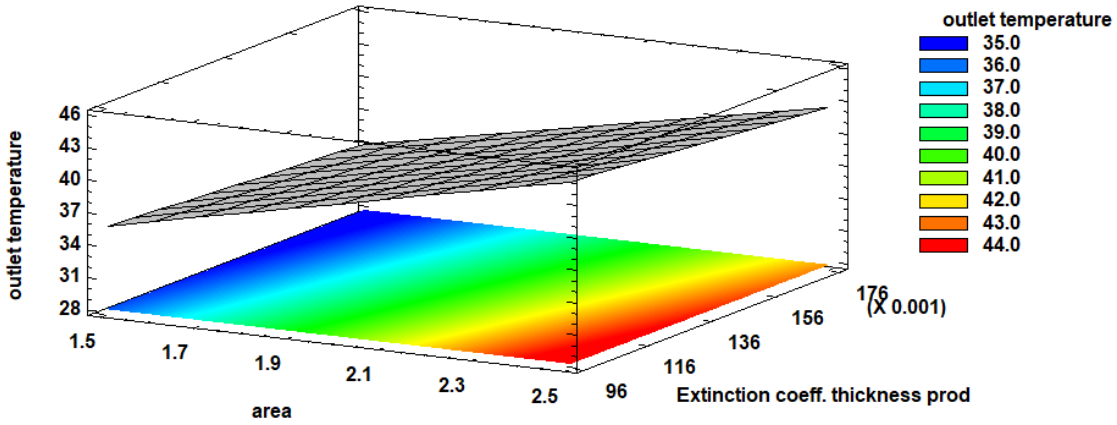

Figure 4.15: Estimated Response Surface for the **Outlet Temperature** as function of Area and Extinction coeff. Thickness and other factors fixed on -1 level

Note Through this figure (4.15), the temperature in the Red zone is 44℃ in the range $[2.15-2.5]m^2$ of Area and $[0.096-0.16]$ of Extinction coeff. Thickness prod, for the green zone the temperature is 32.5℃ in the range $[1.65-2.4]m^2$ and $[0.096-0.16]$, And in the case of the blue zone the outlet temperature is 28℃ in the range $[1.5-1.85]m^2$ and $[0.096-0.16]$.

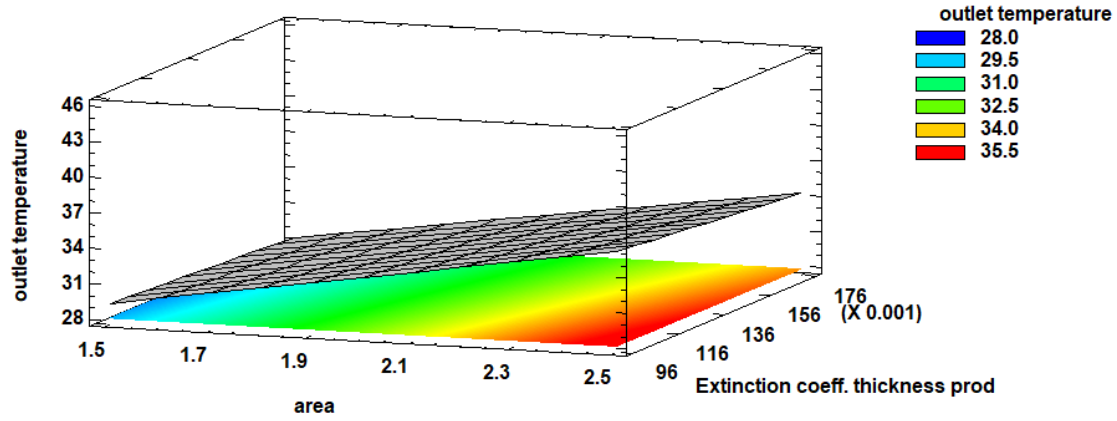

Figure 4.16: Estimated Response Surface for the **Outlet Temperature** as function of Area and Extinction coeff. Thickness and other factors fixed on +1 level

Note Through this figure (4.16), the temperature in the Red zone is 35.5℃ in the range $[2.15 - 2.5]m^2$ of Area and $[0.096 - 0.16]$ of Extinction coeff. Thickness prod, for the green zone the temperature is 32.5℃ in the range $[1.65 - 2.1]m^2$ and $[0.096 - 0.16]$, And in the case of the blue zone the outlet temperature is 28℃ in the range $[1.5 - 1.75]m^2$ and $[0.096 - 0.16]$.

3- the figure (4.17) and figure (4.18) below shows respectively the outlet temperature as a function of Extinction coeff. thickness and Inlet flow rate, and other factors are fixed on -1 and +1 level.

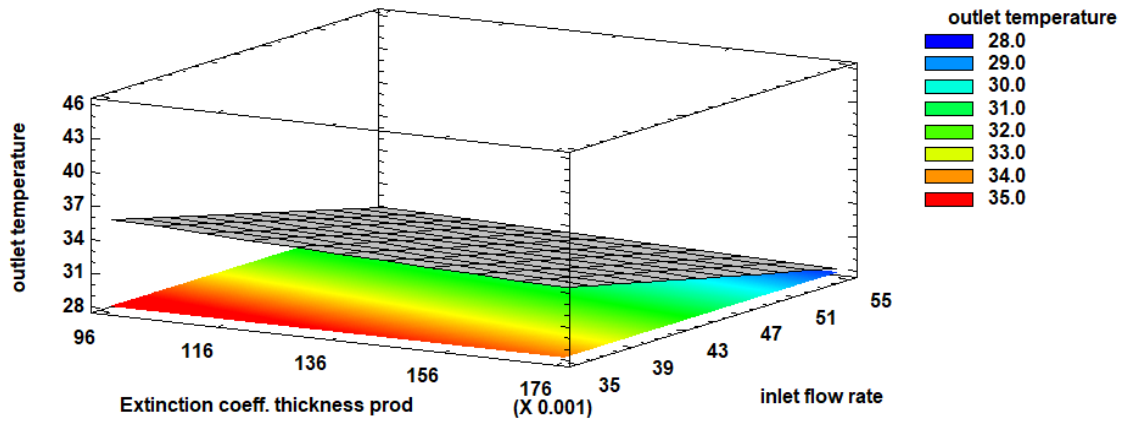

Figure 4.17: Estimated Response Surface for the **Outlet Temperature** as function of Extinction coeff. Thickness and Inlet flow rate, and other factors fixed on -1 level

Note Through this figure (4.17), the temperature in the Red zone is 35.0℃ in the range $[0.096 - 0.16]$ of Extinction coeff. Thickness prod and $[35 - 43]kg/hr$ of Inlet flow rate, for

the green zone the temperature is 32.0℃ in the range $[0.096 - 0.16]$ and $[39 - 53]kg/hr$,and in the case of the blue zone the outlet temperature is 28℃ in the range $[0.096 - 0.16]$ and $[51 - 55]kg/hr$.

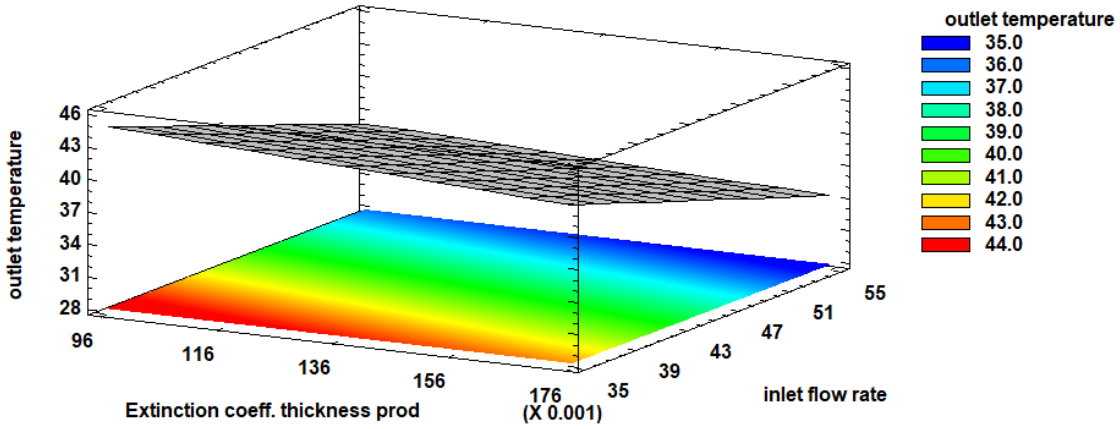

Figure 4. 18: Estimated Response Surface for the **Outlet Temperature** as function of Extinction coeff. Thickness and Inlet flow rate, and other factors fixed on +1 level.

Note Through this figure (4.18), the temperature in the Red zone is 35.0℃ in the range $[0.096 - 0.16]$ of Extinction coeff. Thickness prod and $[35 - 42]kg/hr$ of Inlet flow rate, for the green zone the temperature is 32.0℃ in the range $[0.096 - 0.16]$ and $[42 - 52]kg/hr$, and in the case of the blue zone the outlet temperature is 28℃ in the range $[0.096 - 0.16]$ and $[48 - 55]kg/hr$.

Those figures show the height of the response surface for outlet temperature over the space of Extinction coeff. Thickness and Inlet flow rate, with the other three factors (Area, Index of refraction of cover, Absorptance of absorber) held constant at their high values, over the space of Area and Inlet flow rate, with the other three factors (Extinction coeff. Thickness, Index of refraction of cover and Absorptance of absorber) fixed at their low level and over the space of Area and Extinction coeff. Thickness, whit the other three factors (Inlet flow rate, Index of refraction of cover, Absorptance of absorber) where fixed in the low level.

Then we conclude that the greatest outlet temperature was obtained at high value for Area, low value for Inlet flow rate and low value for Extinction coeff. Thickness and the other factors has little influence it could be set at any value within its experimental range.

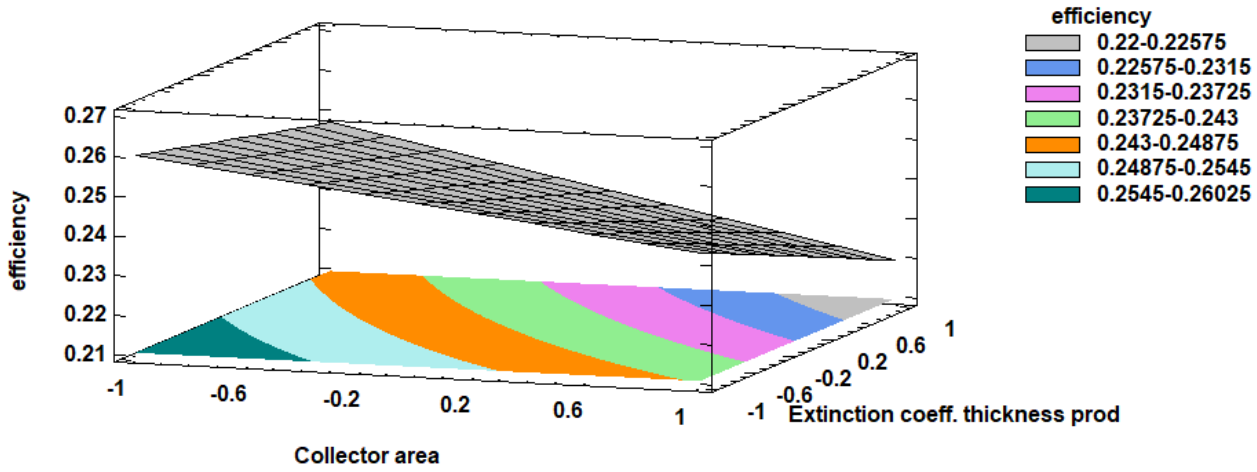

Figure 4. 19: Response surface for the efficiency as a function of the Collector area and Extinction coeff. Thickness prod for fixed values of the Absorptance of absorber plate (-1), Index of refraction of cover (-1) and Inlet flow rate (-1).

This figure clearly indicates that the greatest efficiency was obtained at high values for collector area and high Index of refraction of cover, and low values for Extinction coeff. Thickness, Inlet flow rate and Absorptance of absorber plate.

Figure (4.20) shows an interval for the collector area between the levels '1.5' and '1.8', where the estimated efficiency is 25.2–25.8% when Absorptance of absorber plate, Index of refraction of cover and Inlet flow rate are set at their -1 levels. This plot thus allows the detection of an operating point for optimal performance of the solar air collector,

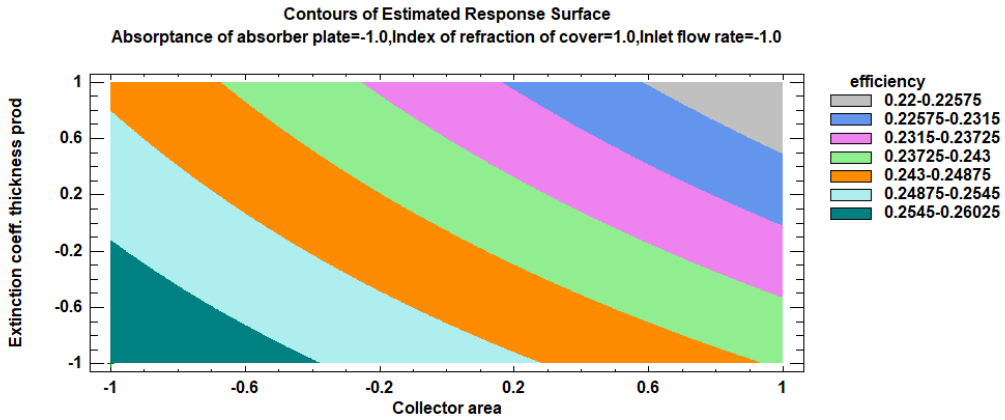

Figure 4. 20: Efficiency ranges as a function of the Collector area and Extinction coeff. Thickness prod for fixed values of the Absorptance of absorber plate (-1), Index of refraction of cover (-1) and Inlet flow rate (-1)

4.4.Finding optimal condition:

In the presence of the magnitude and direction of the variations of the parameters defined, the parameter conditions can be optimized for collector outlet temperature and efficiency. In order to obtain this information, the DOE Wizard uses the concept of desirability functions in order to find a combination of the experimental factors that provides a good result for multiple response variables. "Desirability" is measured on a scale of 0 to 1 whit 1 being the most desirable.

When several responses suggest different optimal operating conditions different optimal operating conditions, a balance between those responses is achieved using desirability functions. The table 4.9 and table 4.10 below shows the estimated response at the optimal settings of the experimental factors.

Table 4.9: Response Values at **Optimum**

Response	Optimized	Prediction	Desirability
outlet temperature	yes	41.4848	0.653346

efficiency	yes	0.24684	

Table 4.10: Factor Settings at Optimum

Factor	Low	High	Optimum
Collector area	1.5	2.5	2.14
Absorptance of absorber plate	0.94	0.95	0.95
Index of refraction of cover	1.49	1.526	1.526
Extinction coeff. thickness prod	0.096	0.16	0.096
Inlet flow rate	35	55	35

For the outlet temperature and efficiency in winter, it is estimated that the maximum percent degree will equal $41.85℃$ and for 0.25 when the factors are set at Area = $2.14\,m^2$, Absorptance of absorber = 0.94, Index of refraction of cover =1.526 it means the glass, Extinction coeff. thickness prod = 0.096, and inlet flow rate = $35\ kg/hr$.

4.5. Simulation of the Solar collector:

4.5.1. Temporal variations of the inlet and outlet temperatures of the collector and of the Radiation global Solar:

The solar radiation which our simulation was run with are illustrate in the Figure (4.21) for the cloudy and summer days. The solar radiation for the winter day is very low and poor that mean that solar energy is not enough for giving fit outlet temperature, in contrary for the summer day it’s same that the solar system (solar energy) can be pass the needs.

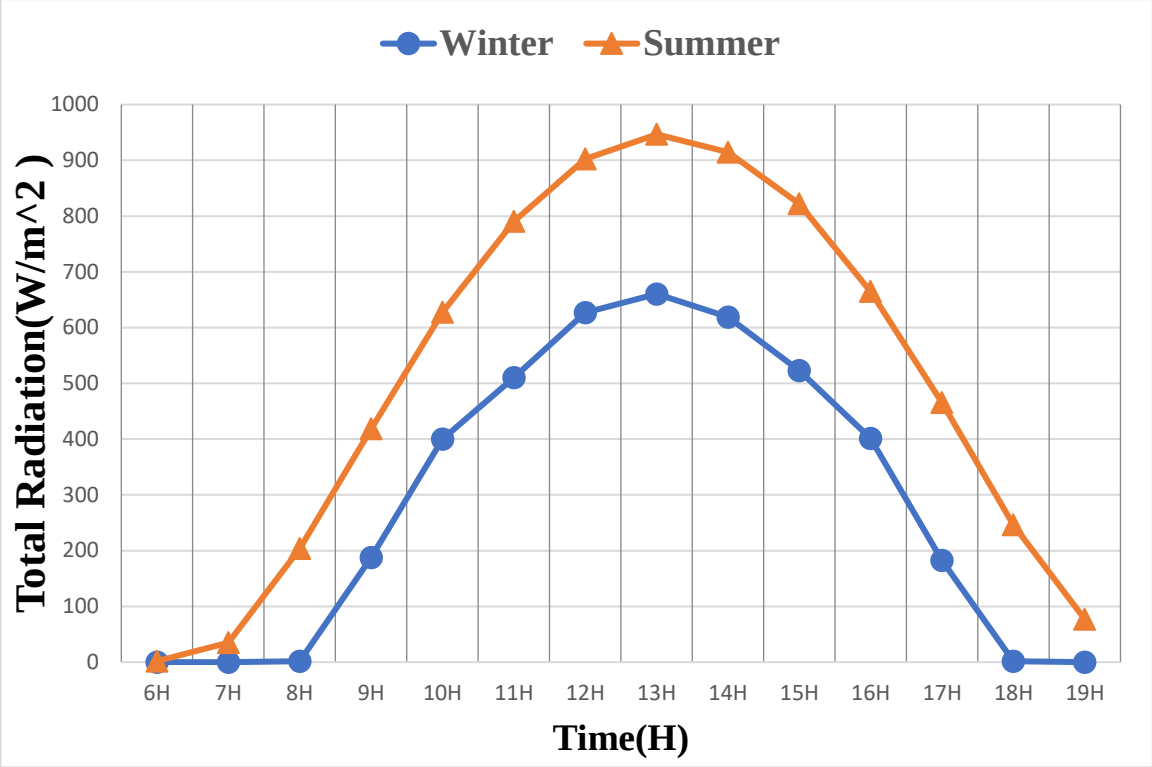

Figure 4. 21: Solar radiation from the site of **Ouargla** for the two typical days

4.5.2. Variation of efficiency in function of the variance of outlet and ambient temperature and total radiation:

The curve illustrates the variation of optimal collector efficiency in function of the ambient temperature of the weather and optimal outlet temperature of the collector and the total solar radiation within 9 hours, it shows us that efficiency of the collector changes inversely in function of temperature change and solar radiation, where it is at its maximum value 32% at 9h and 17h, where the temperature and the solar total radiation is at their lowest value 16.83C° at 9h, 25.57 °C at 17h and 113 W/m^2at 9h and 102.64 W/m^2 at 17h while the efficiency reaches its lowest value 23.5% at 13 hour, it is the peak hour for the temperature and total solar radiation. We interpret that all solar radiation and temperature were greater the lower the rate of efficiency.

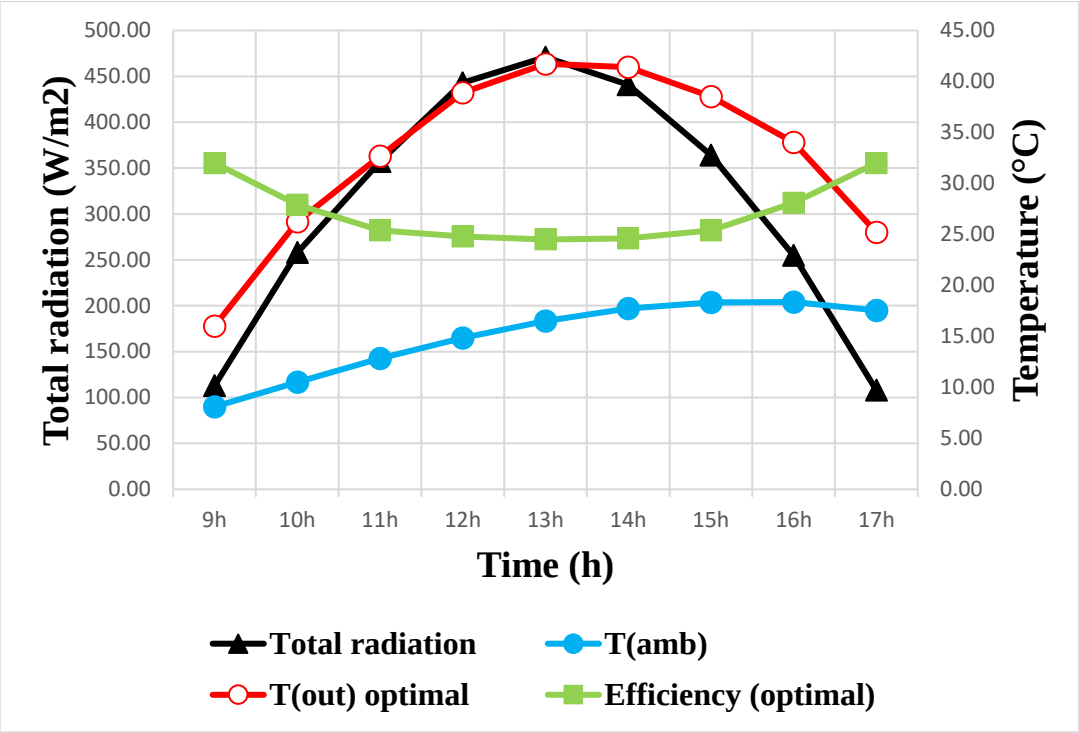

Figure 4. 22: Variation of **Efficiency** in function of **outlet temperature** and total solar radiation in 2th, December 2017.

4.5.3. Comparison between Efficiency rate in summer and winter

In those graph figure (4.23) and (4.24), shows clear variation in how the efficiency change during the summer and winter, where the efficiency in summer up to 15% in great radiation, in contrast, the efficiency in winter is higher in periods of weak radiation rate up to 32% and goes down when the radiation rate is high.

We explain that in summer solar radiation is greater than in the winter and this is shown in figure (4.20), when solar radiation rate rises will lead to increase the temperature in the solar collector and thus increase the rate of used thermal energy (Q_u) so increases the efficiency of the solar collector. In winter, be acquired thermal energy (solar radiation * absorber plate area) is greater than the used thermal energy, because rise in temperature of the solar collector is low than the increasing of solar radiation, as a result of heat loss caused by low weather ambient temperature.

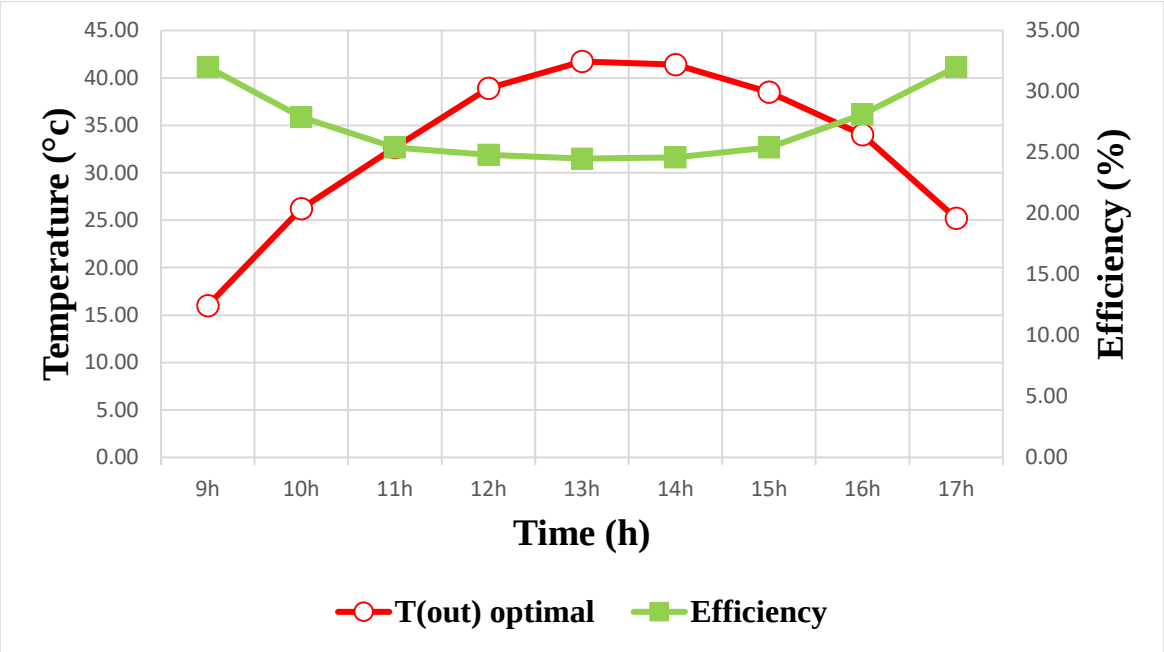

Figure 4. 23: Variation of **efficiency** in function of outlet temperature in winter, the day of 2th December 2017.

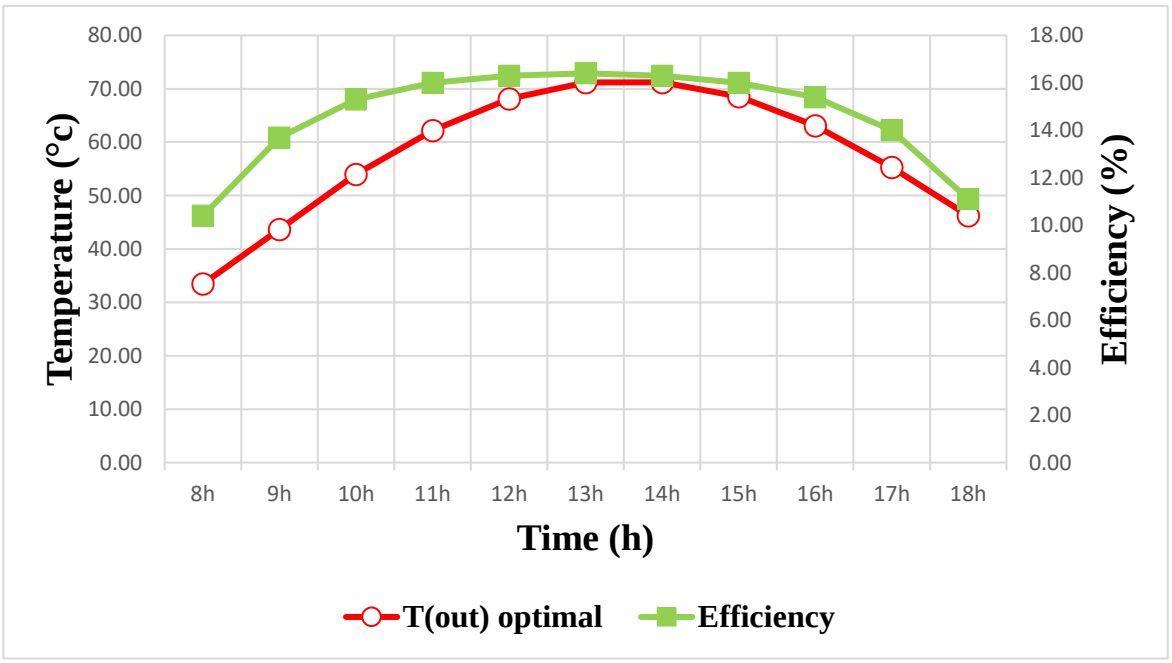

Figure 4.24: Variation of the **efficiency** in function of the outlet temperature in summer the day of 1th, Jun 2017.

4.5.4. Variation of the optimal outlet temperature in function of total solar radiation and ambient temperature:

The curve illustrates the variation of optimal outlet temperature of the solar collector in function of total radiation and ambient temperature within 24 hours. We note that the optimal simulated outlet temperature reaches its peak to 46.46°C at 13h in 938.6 $kJ/h.m^2$ of total solar radiation, during that period of time, we interpret that all solar radiation was greater the higher the rate of collector absorption of radiation and this would lead to an increase in the outlet temperature of the collector

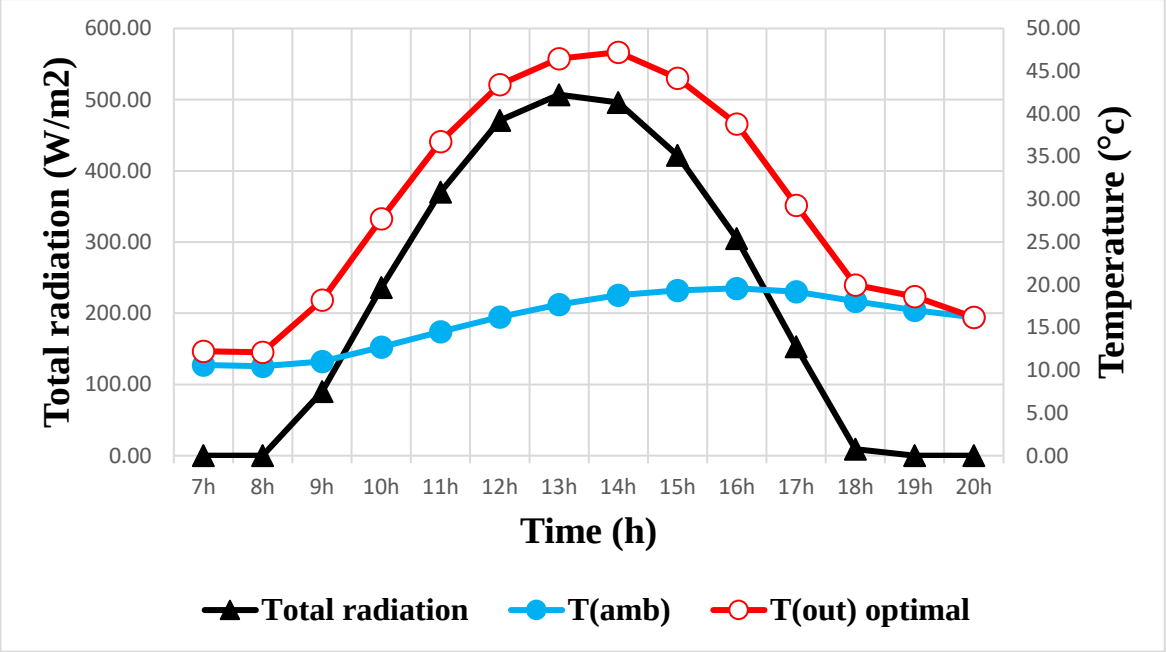

Figure 4.24: Variation of the **outlet temperature** in function of total radiation and ambient temperature in the day of ,1th of January 2017

4.5.5. Variation of the temperature in Temperature in days of different months:

In this graph illustrates how optimal outlet temperatures of the simulated collector change in terms of some months of the year that represent the four seasons where the heat reaches the peak in the summer in the day of 18th Jun to 78 ° C. and in winter 56 °C in the day of 15th December.

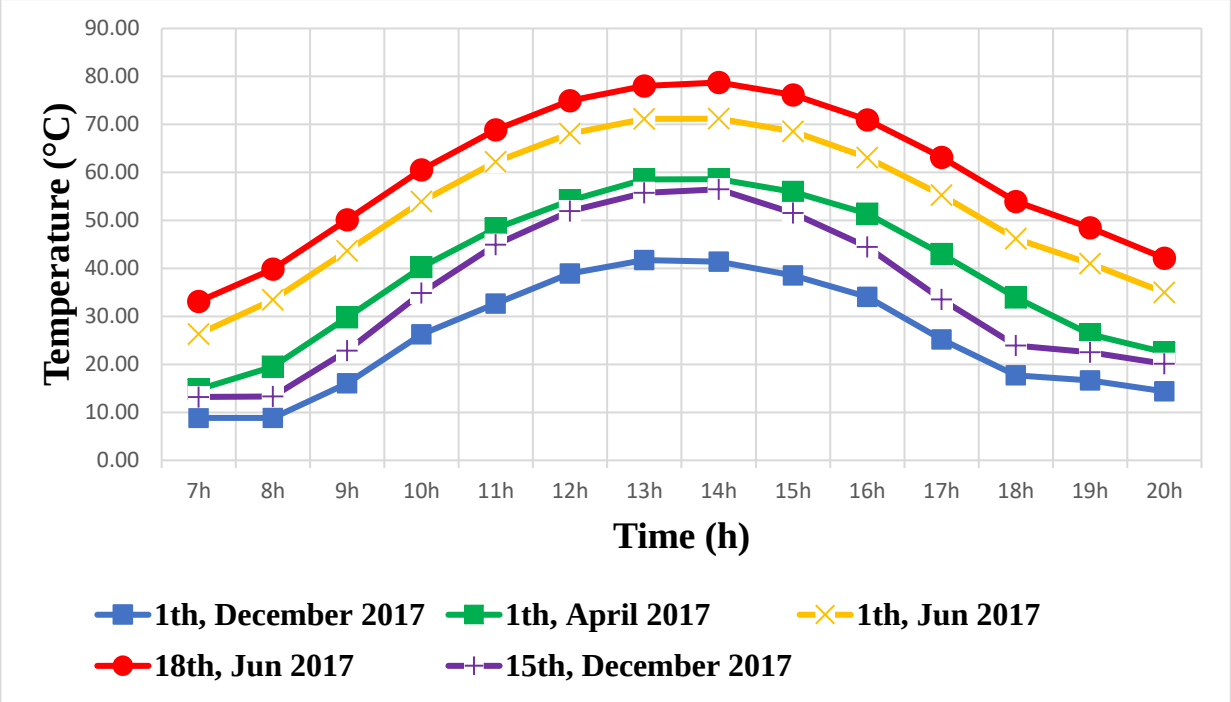

Figure 4.25: Variation of the **outlet temperature** in days of different months

4.5.6. Comparison between optimal and experimental (L.E.N.R.E.Z.A) collector outlet temperature

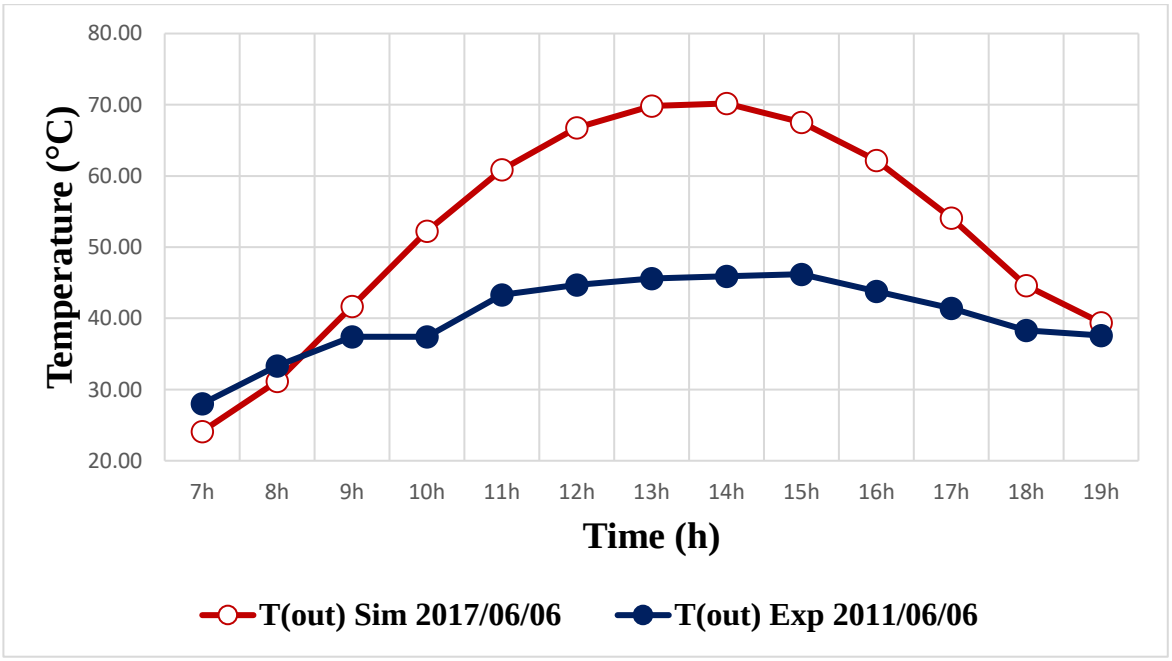

Figure 4.26: Comparison of optimal **outlet temperature** with experimental results in the day of the 06th, Jun

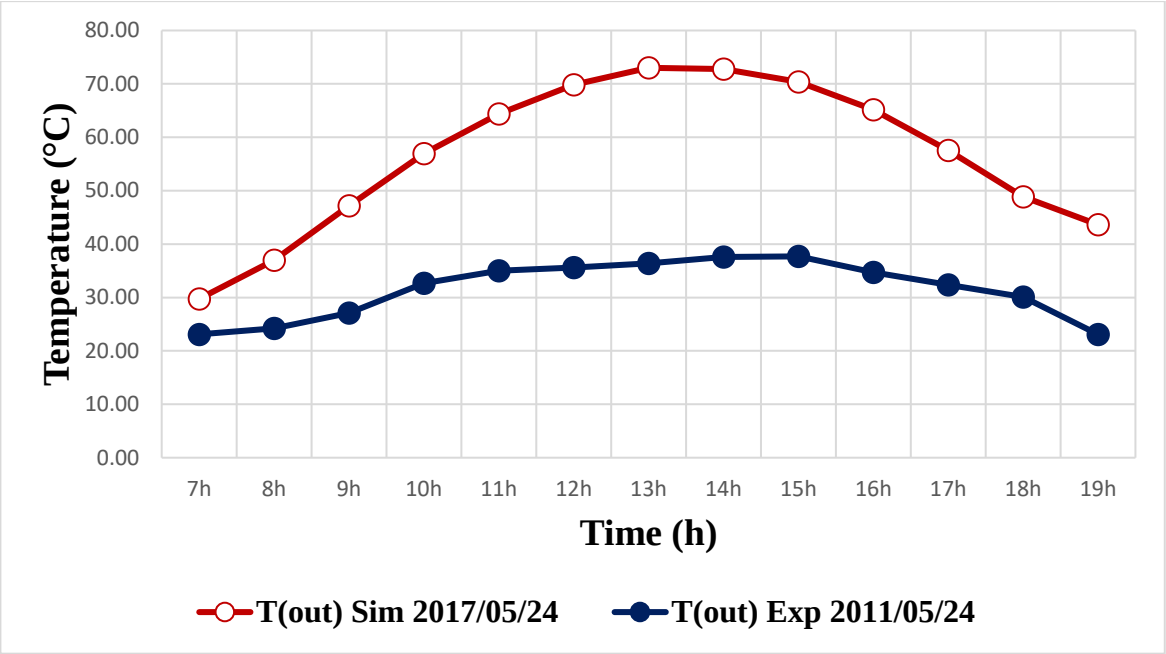

Figure 4.27: Comparison of optimal **outlet temperature** with experimental results in the day of the 24th, May

We note the difference in the temperature of the solar collector is shown in the figure (4.27) and also figure (4.28). Among the results obtained the simulants of factors (optimal) with the results of experimental truth detective (L.E.N.R.E.Z.A) in summer.

There are many reasons for high temperature of simulation results by factors (optimization) weathering results, including the following reasons.

First climate factor is that there is a difference in solar radiation during 2011 and 2017 because it plays an important role in high and low temperature, as well as (the area and thickness of the glass, the type of glass used and the type of absorbent pad, and finally flow). These conditions led to a rise in high temperature.

General conclusion:

The present work aimed to improve the performances of the flat plate solar air collector, especially in the winter, where solar radiation is reduced which negatively affects the outlet temperature of the collector, as well as the low ambient temperature. In order to resolve this problematic we have carried out coupling process between the TRNSYS and STATGRAPHICS software.

First we started a numerical simulation using the TRNSYS software, and we chose the **type73** offered by the program, which is the appropriate type of this study compared to the rest of the types available in the program library. In order to validate the type, we have compared its results with the results that have been piloted by LENREZA laboratory research team, so we subjected the 73 type to the same conditions (climatic and design), where the practical experience was performed. The obtained results showed the authenticity of the simulation model using type 73.

We then moved to the main part of our work, which is to study the factors influencing the outlet temperature and efficiency of the solar collector by using the design of experiments method through Statistical software. A half-fraction scheme was chosen in order to study the effect of the following factors: area, absorptance of absorber plate, index of refraction of cover, inlet flow rate, Extinction coefficient thickness product. The effects of interactions between them on the two responses, outlet temperature and efficiency, coming out of the simulated solar collector using the TRNSYS program depending on type 73, were also studied. The results issued from the design of experiment, given by the Pareto chart show that both the area and air flow are the most influential factors in outlet temperature and observed that their effect on outlet temperature is different as the effect the area is positive the flow effect is negative. For the efficiency the pareto chart shows that there is three influential factors which are collector area, Extinction coeff. Thickness prod and inlet flow rate, which we have a negative influence of both of collector area, Extinction coeff. Thickness prod. Whereas a positive influence of inlet flow rate, as (interaction) shows, the extent to which factors interaction and their impact on outlet temperature and efficiency is observed to be the most obvious interaction was between the collector area and the inlet flow rate where the effect of the collector area on outlet temperature is large at the lowest flow value, which is more pronounced by what it shows (response surface). Regarding the efficiency, the most obvious interaction between collector area and ‘extinction coefficient Thickness prod’ where the effect of the collector area on efficiency is high at the low level of ‘extinction coefficient Thickness prod’.

The optimisation process gave the final result of the optimal conditions at which the outlet temperature and efficiency of the flat plat solar air collector are at maximum values. These results were as follows: the area 2.14 m^2, the absorber plate type is the copper, the type of glass is normal glass (which is more permeable to solar rays than the Plexiglass), Inlet flow rate 35 kg/hr (an important factor in increasing the outlet temperature), 3 mm thickness of the glass, which allows the maximum possible value of solar radiation to pass through the glass.

Then in the last step of the study we did a numerical simulation of the solar collector using the TRNSYS software, based on the optimal conditions, and comparing the results by the results of the practical experience in the LENREZA laboratory and our eagerness to be in the same climatic conditions, depending on the METEONORM software. The results, using the optimal conditions that we have extracted in the way of design of experiments, showed a noticeable improvement in thermal behaviour represented in the outlet temperature compared to the tests previously carried out in the LENREZA laboratory, where the outlet temperature arrived at (13:00) in the day of 2^{th} December to 41.85 °C while the efficiency reaching to 0.25. Finally, figures illustrating the work of the modelled solar collector during different months were presented and commented.

References:

[1] site web: http://www.eldjazaircom.dz/index.php?id_rubrique=347&id_article=4176

[2] INSHA, Mohd. EXPERIMENTAL STUDY ON PERFORMANCE OF A DOUBLE PASS SOLAR AIR HEATER. 2016.

[3] BOUDKHIL, AFFANE. Développement d'un outil d'optimisation multicritère des systèmes solaires thermiques pour des besoins d'une habitation. Thèse de doctorat., 2014,

[4] AMOABENG, Owura Kofi. Assessing the feasibility of a solar water heating system based on performance and economic analysis. 2012. Thèse de doctorat.

[5] IORDANOU, Grigorios. Flat-plate solar collectors for water heating with improved heat transfer for application in climatic conditions of the Mediterranean region. 2009. Thèse de doctorat. Durham University.

[6] AES-L2."solar collectors", 2017, p 4. Sit web: http://users.fs.cvut.cz/tomas.matuska/wordpress/wp-ontent/uploads/2015/02/AES- L2-solar_collectors_2017.pdf

[7] KASSA, Adane. INVESTIGATION OF PARABOLIC DISH SOLAR CONCENTRATOR FOR LOCAL AREKE DISTILLATION. 2015. Thèse de doctorat. Addis Ababa University.

[8] JAE-MO KOO, "development of a flat-plate solar collector design program " a thesis submitted in partial fulfillment of the requirements for the degree of master of science (mechanical engineering) at the university of Wisconsin Madison 1999

[9] AMRAOUI, Mohammed Amine. Numerical Study of the Three-dimensional Flow in a Flat Plate Solar Collector with Baffles. S01 Modélisation avancée en mécanique des solides et des fluides, 2015.

[10] SOBHANSARBANDI, Sarvenaz. Performances of Flat-Plate and CPC Solar Collectors in Underfloor Heating Systems. 2013. Thèse de doctorat. Eastern Mediterranean University (EMU).

[11] Sit web : http://www.paksolarservices.com/solar-heat-collector.html

[12] VYAS, Santosh et PUNJABI, Dr Sunil. Thermal Performance Testing of a flat Plate Solar Air Heater Using Optical Measurement Technique. International Journal of Recent advances in Mechanical Engineering (IJMECH), 2014, vol. 3, no 4.

[13] ION, V. I. et MARTINS, G. J. Design, developing and testing of a solar air collector. The annals of «Dunarea de Jos» University of Galati Fascicle IV Refrigerating technique, internal combustion engines, boilers and turbines. 2006.

[14] KALOGIROU, S. A., LLOYD, S., WARD, J., et al. Design and performance characteristics of a parabolic-trough solar-collector system. Applied energy, 1994, vol. 47, no 4, p. 341-354.

[15] K. Salima. ¨Etude théorique et numérique des systèmes couples : distillateur plan capteur et distillateur hot box-capteur¨. Thèse de magister (2009) 03-15.

[16] TIBEBU, Tiruwork Berhanu. Design, construction and evaluation of performance of solar dryer for drying fruit. 2015. Thèse de doctorat.

[17] SANDALI, Messaoud. Etude dynamique et thermique d'un capteur solaire à air à double passe avec milieu poreux. 2014. Thèse de doctorat.

[18] ABABSA, Dalila. Optimisation du rendement d'un capteur solaire par minimisation des pertes convectives. 2009. Thèse de doctorat. Thèse de magister Université Batna.

[19] SOUAD, SAADI. Effet des paramètres opérationnels sur les performances d'un capteur solaire plan. UNIVERSITE MENTOURI DE CONSTANTINE, 2010, vol. 2, no 51, p. 3.

[20] DOMÍNGUEZ-MUÑOZ, Fernando, ANDERSON, Brian, CEJUDO-LÓPEZ, José M., et al. Uncertainty in the thermal conductivity of insulation materials. Energy and Buildings, 2010, vol. 42, no 11, p. 2159-2168.

[21] SYAHRUL, S., HAMDULLAHPUR, F., et DINCER, I. Exergy analysis of fluidized bed drying of moist particles. Exergy, an International Journal, 2002, vol. 2, no 2, p. 87-98.

[22] ISOPENCU, Gabriela, MARES, Alina Monica, et JINESCU, Gheorghita. Energy and Exergy Studies for Different Intensifying Processes of Malt Drying. REVISTA DE CHIMIE, 2017, vol. 68, no 6, p. 1274-1280.

[23] BEJAN, Adrian. Advanced engineering thermodynamics. John Wiley & Sons, 2016.

[24] EKECHUKWU, O. V. Review of solar-energy drying systems I: an overview of drying principles and theory. Energy conversion and management, 1999, vol. 40, no 6, p. 593-613.

[25] SHARMA, Atul, CHEN, C. R., et LAN, Nguyen Vu. Solar-energy drying systems: A review. Renewable and sustainable energy reviews, 2009, vol. 13, no 6-7, p. 1185-1210.

[26] BELESSIOTIS, V. et DELYANNIS, E. Solar drying. Solar energy, 2011, vol. 85, no 8, p. 1665-1691.

[27] CHAIGNON, Juliette. Modeling of a solar dryer for fruit preservation in developing countries. 2017.

[28] Sharma, A., Chen, C.R. and Vu Lan, N. "Solar-drying systems: a review". In: Renewable and Sustainable Energy Reviews 13, pp. 1185–1210, 2009.

[29] EL-LAMUSHE, Hassan Yousef. A numerical and experimental study of a photovoltaic powered solar rice dryer. 1999.

[30] KUMAR, Mahesh, SANSANIWAL, Sunil Kumar, et KHATAK, Pankaj. Progress in solar dryers for drying various commodities. Renewable and Sustainable Energy Reviews, 2016, vol. 55, p. 346-360.

[31] EKECHUKWU, O. Va et NORTON, Brian. Review of solar-energy drying systems II: an overview of solar drying technology. Energy conversion and management, 1999, vol. 40, no 6, p. 615-655.

[32] BERREBEUH Mouhamed Hafed, "Maturation artificielle des dattes par étuvage. Effets des transferts thermo-massiques sur la qualité du fruit". These doctoral in Sciences. University Kasdi Merbah Ouargla faculte of sciences appliquees.2017.

[33] VRANIC, Branko Z. Design of experiments methodology in studying near-infrared spectral information of model intact tablets: simultaneous determination of metoprolol tartrate and hydrochlorothiazide in solid dosage forms and powder compressibility assessment using near-infrared spectroscopy. 2015. Thèse de doctorat. University_of_Basel.

[34] StatPoint ."STATGRAPHICS Centurion XVI User Manual" .StatPoint Technologies, Inc, 2009 sit web: www.STATGRAPHICS.com

[35] https://www.moresteam.com/toolbox/design-of-experiments.cfm

[36] STATGRAPHICS. "DOE Wizard – Screening Designs ".StatPoint Technologies, Inc,2017. Sit we:b: www.STATGRAPHICS.com

[37] Davies, N. and Tremayne, A. R. (1994), Review of statgraphics. J. Appl. Econ., 9: p335-341. doi:10.1002/jae.3950090308

[38] Sit web: https://www.qualitydigest.com/jan02/html/software.html

[39] WALTZ, James P. Computerized building energy simulation handbook. CRC Press, 2000.

[40] BEGGAA, Lalmi et GHERIER, Said. IMPACT DE LA FORME ARCHITECTURALE SUR LA PERFORMANCE ENERGETIQUE. 2017. Thèse de doctorat.

[41] BENMEHDI, RACHID. Conception et régulation des systèmes fermés de distribution et de circulation de chauffage/climatisation. 2014. Thèse de doctorat.

[42] TRNSYS, "TRNSYS 17 Reference Manual," Solar Energy Laboratory, University ofWisconsin-Madison, 2012.

[43] MOGHARBI Mohamed and HALASSA Daoud, " Conception et réalisation d'un capteur solaire plan à air", mémoire de fin d'études pour l'obtention du diplôme de master, Université Kasdi MERBAH de OuarglaFaculté des sciences technologie et sciences de la matièreDépartement de Génie mécanique, 2010.

[44] Siteweb:https://www.ecse.rpi.edu/~schubert/Educational-resources/Materials-Refractive-index-and-extinction-coefficient.pdf," Refractive index and extinction coefficient of materials",2004.

[45] BADACHE, Messaoud. Étude numérique et expérimentale du transfert de chaleur dans un capteur solaire à perforations doté d'un collecteur transparent et opaque. 2013. Thèse de doctorat. École de technologie supérieure.

الملخص

ركزت الدراسة الحالية على أمثلة اللاقط الشمسي الهوائي بهدف تحسين الكفاءة الطاقوية من خلال إجراء عدد من تجارب المحاكاة العددية إعتمادا على برنامج TRNSYS لدراسة الكفاءة الطاقوية وبرنامج STATGRAPHICSللأمثلة الرياضية وذلك بهدف البحث عن الشروط المثالية للعوامل المؤثرة على كفاءة اللاقط الشمسي.

من أجل الحصول على كفاءة مثالية للاقط استعملنا طريقة مخططات التجارب التي تعطي نتائج تحليلية سليمة وموضوعية بدل التجارب الإنتاجية التقليدية. بعد المقارنة مع النتائج التجريبية، تم الحصول على نتائج مرضية في هذه الدراسة. علاوة على ذلك، وجد أن الكفاءة الطاقوية للاقط بإستعمال الشروط المثالية التي استخرجناها بطريقة مخططات التجارب تحسنت تحسنا ملحوظا مقارنة بالتجارب التي أجريت من قبل في مخبر تطوير الطاقات الجديدة و المتجددة في المناطق الجافة و الصحراويةLENREZA .

كانت أفضل الشروط من أجل درجة حرارة و كفاءة مثاليين، المساحة 2.14م^2، نوع السطح الماص هو الحديد غير قابل للصدء، نوع الزجاج هو (الزجاج العادي)، التدفق الهوائي 35 كغ/سا ويعتبر عامل مهم في زيادة درجة الحرارة، سمك الزجاجة 3 مم حيث يسمح بمرور أكبر قيمة ممكنة من الإشعاع الشمسي عبر الزجاج، حيث وصلت درجة الحرارة في فصل الشتاء إلى 41.86 درجة و كفاءة اللاقط 25%، في حين تصل في فصل الصيف إلى75 درجة بكفاءة 16%.

الكلمات المفتاحية: اللاقط الشمسي ، درجة الحرارة الخارجة ، مخططات التجارب ، الأمثلة الرياضية

Abstract

The present study focused on the optimization of flat plane solar air collector, to improve its thermal performance, by conducting a number of numerical simulation experiments based on the TRNSYS software for the study of energy efficiency and STATGRAPHICS for mathematical modeling in order to find the ideal conditions for the factors affecting the efficiency of the solar collector.

In order to obtain optimal efficiency of the collector, we used the experimental design method that gives correct and objective analytical results instead of the traditional procedure of experiments. After making some comparisons with the experimental data, satisfactory results were obtained in this study. In addition, it was found that the energy efficiency of the collector using the optimal conditions, extracted in the experimental design method, improved significantly compared with the previous experiments conducted at LENREZA laboratory. The best conditions for optimum outlet temperature and efficiency were as: 2.14 m^2 area, absorbent surface type stainless steel, glass type normal glass, air flow 35 kg / h which is an important factor in increasing temperature, glass thickness 3 mm allowing the maximum possible amount of solar radiation. The outlet temperature in the winter reaches 41.86 °C and the efficiency of the collector 25%, while in the summer it reaches 75°C with efficiency of 16%.

Résumé

La présente étude a porté sur l'optimisation du capteur solaire plan à) air, afin d'améliorer ses performances thermiques, en réalisant un certain nombre d'expériences de simulation numérique basées sur le logiciel TRNSYS pour l'étude de l'efficacité énergétique et STATGRAPHICS pour la modélisation mathématique menant aux conditions idéales pour les facteurs affectant l'efficacité du capteur solaire. Afin d'obtenir une efficacité optimale du capteur solaire, nous avons utilisé la méthode des plans d'expériences qui donne des résultats analytiques corrects et objectifs, en alternative à la procédure d'expérimentation classique. Après quelques comparaisons avec les données expérimentales, des résultats satisfaisants ont été obtenus dans cette étude. En outre, il a été constaté que l'efficacité énergétique du capteur solaire, en utilisant les conditions optimales extraites dans la méthode des plans d'expériences, s'est améliorée de manière significative par rapport aux expériences précédentes menées au laboratoire LENREZA. Les meilleures conditions pour une température de sortie et une efficacité optimales étaient telles que : surface de 2.14 m^2, type de surface absorbante en acier inoxydable, verre type verre normal, débit d'air 35 kg / h qui est un facteur important pour augmenter la température, épaisseur de verre 3 mm offrant une quantité maximale de rayonnement solaire traversant. La température de sortie en hiver atteint 41,86 °C et l'efficacité du collecteur 25%, tandis qu'en été, elle atteint 75°C avec un rendement de 16%.